Check for updates

Electromagnetic bioeffects: a multiscale molecular simulation perspective

Benjamin B. Noble, [ID] [ab] Nevena Todorova [ID] [ab] and Irene Yarovsky [ID] ⋆[ab]

Electromagnetic bioeffects remain an enigma from both the experimental and theoretical perspectives despite the ubiquitous presence of related technologies in contemporary life. Multiscale computational modelling can provide valuable insights into biochemical systems and predict how they will be perturbed by external stimuli. At a microscopic level, it can be used to determine what (sub)molecular scale reactions various stimuli might induce; at a macroscopic level, it can be used to examine how these changes affect dynamic behaviour of essential molecules within the crowded biomolecular milieu in living tissues. In this review, we summarise and evaluate recent computational studies that examined the impact of externally applied electric and electromagnetic fields on biologically relevant molecular systems. First, we briefly outline the various methodological approaches that have been employed to study static and oscillating field effects across different time and length scales. The practical value of such modelling is then illustrated through representative case-studies that showcase the diverse effects of electric and electromagnetic field on the main physiological solvent – water, and the essential biomolecules – DNA, proteins, lipids, as well as some novel biomedically relevant nanomaterials. The implications and relevance of the theoretical multiscale modelling to practical applications in therapeutic medicine are also discussed. Finally, we summarise ongoing challenges and potential opportunities for theoretical modelling to advance the current understanding of electromagnetic bioeffects for their modulation and/or beneficial exploitation in biomedicine and industry.

Introduction

The interaction of biomaterials with electric fields (EFs) and electromagnetic fields (EMFs) has attracted increasing attention over the last few decades, due to increased recognition of the importance of the external fields in modulating structure and activity of biomolecules[1–8] as well as emerging EF and EMF applications in therapeutic medicine.[9–13] On-going research efforts addressing several important aspects of the EMF health debate including the mechanisms, neurodegenerative diseases, cancer and exposure dosimetry, have been summarised in several reviews.[14–16] In 2015 English and Waldron provided a detailed perspective on the progress and challenges of molecular simulations of external EFs, as well as the potential impact and prospects for exploitation of such simulations for real-world and industrial applications.[17] More generally, the effect of static EFs on chemical reactivity has been discussed in several reviews and perspectives.[18–21] A recently published book on this topic[22] provides an excellent and detailed overview of the EM/EMF effects on structure and reactivity, including applications and recent theoretical developments in EF-mediated chemistry.

In this review, we outline how multiscale theoretical methodology can be used to study the impacts of external EF and EMF on the electronic and atomistic structure of biologically relevant molecules and their assemblies in physiological environments. We present a theoretical background of quantum chemical and classical modelling approaches that are used to study the effect of external fields on biomolecular systems. Next, we examine recent literature to highlight how multiscale computational modelling can be used to explore the effects of external EFs (and EMFs) on physiologically relevant biomolecular systems, including aqueous solutions, DNA, proteins and enzymes, membranes and biomedically important nanomaterials.

Sufficiently intense EF and EMF can influence both the structure and reactivity of (bio)molecules. These effects can include altering equilibrium geometries[23] and molecular spectroscopy (*e.g.* the Stark and Zeeman effect) as well as altering electron[24,25] and H-atom[26] transfer and bond cleavage/reformation processes.[27–30] Indeed, the highly specific orientation of charged and polar residues within enzymes naturally creates local EFs that are often necessary for their function.[25,31,32] Given this, it is worth briefly distinguishing between different types of EF and EMF that are encountered within the context of (bio)chemical modelling:

[a] *School of Engineering, RMIT University, GPO Box 2476, Melbourne, Australia.*
  E-mail: irene.yarovsky@rmit.edu.au
[b] *Australian Centre for Electromagnetic Bioeffects Research, Australia*

This journal is © the Owner Societies 2022

Phys. Chem. Chem. Phys., 2022, **24**, 6327–6348 | **6327**

• External static electric fields are uniform with respect to time (and generally space) and are generated by a voltage bias (*e.g.* within a capacitor, scanning tunnelling microscopy or a charged surface).

• External oscillating electromagnetic fields (electromagnetic radiation) oscillate in both time and space, generally propagating at the speed of light through a given medium. The period of these oscillations (or conversely their wavelength) determines the energy carried by these fields and consequently they are normally categorised as either ionizing or non-ionizing depending on their ability to ionize biomolecules and/or break chemical bonds.

• Local or intrinsic electric fields are generated from orientated dipoles, and ions within molecular systems (*e.g.* biological membranes, at enzyme active sites) and are essentially inherent. These EFs can fluctuate with time depending on the specific molecular configuration(s) within the system.

As molecules can be viewed as ensembles of charged elementary particles, the molecular systems can be perturbed by external EFs. However, as large intrinsic fields often occur spontaneously within chemical systems, relatively intense external EFs are generally required to observe significant chemical or physical effects. For context, Table 1 compares the peak magnitudes of external EFs that can be generated by various sources to those of intrinsic fields that occur naturally within (bio)chemical systems.

As Table 1 outlines, the intrinsic EFs experienced by electrons within a typical molecule are surprisingly large and can easily exceed 10^2 V nm^{-1}, particularly close to the nucleus. Moreover, many biomolecular structures (*e.g.* DNA, proteins and membranes) generate significant intrinsic fields on the order of 1 V nm^{-1}. In contrast, external EFs that are generated within houses and offices by consumer electronics are typically of the order 10^{-7} V nm^{-1}. However, higher-intensity (typically $|E| > 10^{-5}$ V nm^{-1}) and short duration (ranging from microseconds to nanoseconds) pulsed EFs have been utilised for various therapeutic applications. The applications include treating melanoma[38] and cutaneous tumours implanted in mice,[39] as well wound healing[40,41] and tissue ablation.[42] In general, these applications operate through the formation of nanoscale defects in the cell membrane (electroporation) that are within the timescale of current modelling capabilities. There has also been substantial interest in the effects of static and time-varying EFs on protein conformation,[3–8,46–54] as the formation of insoluble aggregates (amyloid fibrils) are thought to contribute to the onset of various neurodegenerative diseases (*e.g.* Parkinson's and Alzheimer's).[47,55,56] Intriguingly,

some evidence has been reported of high-frequency EMFs reducing amyloid fibrils in the brain of Alzheimer's patients.[15,57]

Fig. 1 schematically relates the time and length scales accessible to the theoretical modelling techniques associated with various biomolecular systems, physicochemical phenomena and EMF radiation spectrum. Quantum Mechanical (QM) approaches are particularly well suited to the study of bond breaking/forming reactions and are commonly utilised for modelling enzymatic transformations as well as determining chemically accurate interaction energies (*e.g.* for metal–ligand complexes, molecular recognition, drug binding). QM approaches are well suited for studying enthalpically driven processes, which usually involve significant changes in chemical bonding along a well-defined reaction coordinate. The macroscopic descriptors of the processes in question (*e.g.* rate coefficients and equilibrium) can be accurately determined by identifying critical points on the potential energy surface that describe motion along these degrees of freedom (see QM approaches below). QM-based approaches are currently only feasible for relatively small molecular systems and so are limited to biomolecules and biochemical processes that occur on the nanometre scale.

Classically propagated systems using molecular mechanics and dynamics (MD) approaches, where atoms are treated as spring connected (bonded) or disconnected (non-bonded) point charges and many-body interactions are represented by inter-atomic interaction potentials, so called force fields (FFs), are significantly larger (100 000+ atoms) and allow for both static and time-dependent (oscillating) EF to be investigated. All-atom inclusive models simulated by MD enable direct insight into the fundamental EF effects on molecular processes, structure, and dynamics of biological molecules (water, DNA, peptides/proteins, lipid membranes) and materials (nanoparticles, organic and inorganic surfaces) in physiological conditions at spatial and temporal resolutions currently inaccessible by laboratory techniques, and as such have proven to be highly complementary to the experimental efforts in this area.[17,58,59] MD is well suited for studying entropically driven processes, which involve significant changes in the configurations of the system (*e.g.* conformations, solvent orientations) over multiple degrees of freedom. These processes are governed by the probabilities of the system populating different (thermally accessible) microstates, which requires explicit simulation and statistical sampling of these states.

Below we present a theoretical background of quantum chemical and classical modelling approaches and critically

Table 1 Typical exposures from different EF (and EMF) sources and intrinsic EFs encountered within (bio)chemical systems

External fields			Intrinsic fields		
Application/source	$|\mathbb{E}|$ (V nm^{-1})	Ref.	System	$|\mathbb{E}|$ (V nm^{-1})	Ref.
Within typical houses	10^{-8}–10^{-7}	33	Within liquid water	10	34
Below high voltage transmission lines	10^{-6}–10^{-5}	33 and 35	Internal potential within phospholipid membranes	0.1–1	36 and 37
Therapeutic medicine	10^{-5}–10^{-2}	38–42	Within DNA	1	19
Electrode surfaces	10^{-4}–1	19	Transmembrane potential	10^{-2}	36 and 37
Scanning tunnelling microscopy (STM)	1–10	19, 43 and 44	Within typical proteins	0.1–10	19 and 45
Laser fields	>10	19	Electron charge at 0.53 Å	5.1×10^2	19

6328 | *Phys. Chem. Chem. Phys.*, 2022, **24**, 6327–6348
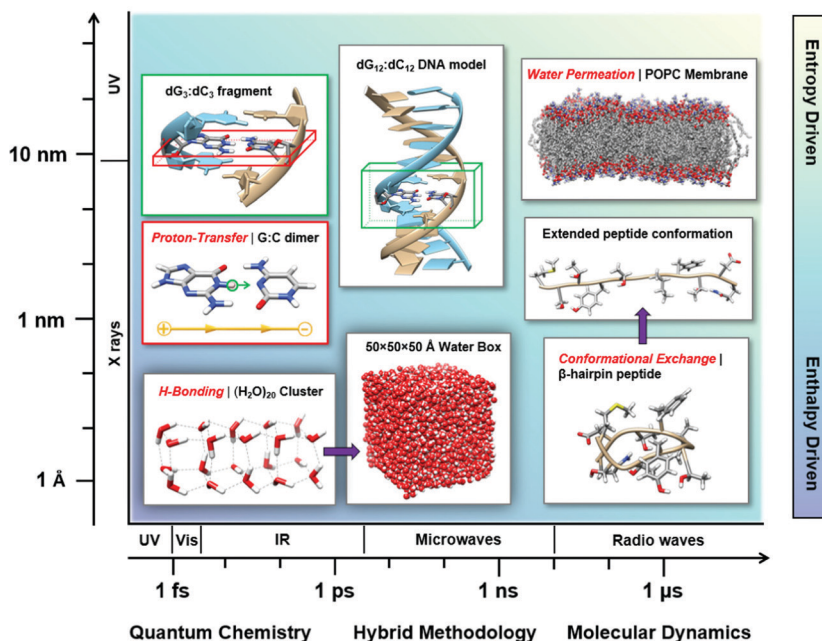
This journal is © the Owner Societies 2022

Fig. 1 Time and length scales accessible to multiscale modelling associated with various biomolecular systems, physicochemical phenomena, and EMF radiation spectrum, illustrated by exemplar studies of the effect of static EFs on proton-transfer in DNA models[60–62] and hydrogen bond structuring in water,[63,64] the impact of EMFs on peptide conformations[64] and water permeation of membranes.[59] Images are not to scale.

review recent literature employing the computational modelling to explore the effect of external EFs (and EMFs) on biomolecular systems. We show how multiscale theoretical approaches can be used to study the impacts of external EF and EMF on the electronic and atomistic structure of biologically relevant molecules and their assemblies in physiological environments of living organisms or within the latest biomedical technologies.

Theoretical background

Quantum mechanical approaches

Quantum mechanical approaches can be categorised depending on how molecular energies/properties are initially calculated (*e.g.* wavefunction theory, density functional theory) and how these calculations are utilised to predict macroscopic observables (*e.g.* free-energies, reaction rates). Many references provide detailed summaries on the calculation of molecular energies and properties as well as their use in predicting macroscopic observables.[65–67] Here we focus on key aspects relevant to condensed-phase multi-scale modelling, contrasting the strengths and weaknesses of different conceptual approaches for modelling static EFs and oscillating EMFs.

Electronic structure calculations for static EFs and EMF response properties

Electronic structure calculations can be used to infer dynamic behaviour, predicting macroscopic observables (*e.g.* rate coefficients, equilibrium constants) *via* critical points on the potential energy surface (PES), the so called 'potential landscape' paradigm of chemical reactivity.[68,69] These geometric features can be used to predict how static EFs influence a (bio)molecular

system along a predetermined reaction coordinate. Meanwhile, both static and dynamic molecular response properties, which describe how systems are perturbed by EMFs of a given frequency, can be approximated by taking various derivatives of the energy and by using perturbative expansions. Non-ionizing radiation carries insufficient energy to promote electronic excitations in (bio)chemical systems. Instead, this radiation excites vibrational and rotational modes of the underlying nuclei. Thus, the wavelength and intensity of these vibrational transitions will determine how a given system interacts with a dynamic (non-ionizing) EMF.

The standard approach for calculating vibrational (and internal rotational) transitions uses Taylor series expansions to describe the PES and molecular interactions with the EMF.[70] Under the 'double harmonic' approximation, these expansions are truncated at second-order coefficients, though inclusion of additional anharmonic response terms provides better accuracy (at increased computational expense). The double harmonic approximation describes nuclear dynamics *via* a 3N system of independent quantum harmonic oscillators, in terms of motion along internal degrees of freedom (or normal coordinates), denoted $Q_1, Q_2,\ldots,Q_{3N} \equiv \boldsymbol{Q}$.[70] Within the Born–Oppenheimer approximation, these vibrational states are found by solving the nuclear Schrodinger equation in terms of these normal coordinates:

$$\mathcal{H}\Psi_s(\boldsymbol{Q}) = E_s\Psi_s(\boldsymbol{Q}) \tag{1}$$

Here $\Psi_s(\boldsymbol{Q})$ is the vibrational wavefunction of the sth vibrational state and E_s is its corresponding energy. By neglecting rotational angular momentum and rotational coupling effects, the

Hamiltonian operator, $\mathcal{H}$, can be written:

$$\mathcal{H} = \sum_{k=1}^{3N} -\frac{1}{2}\frac{\partial^2}{\partial Q_k^2} + V(\boldsymbol{Q}) \qquad (2)$$

Here $V(\boldsymbol{Q})$ is the Born–Oppenheimer PES described in mass-weighted normal coordinates. Because evaluating the full PES across all $3N$ degrees of freedom is often computationally prohibitive, it is approximated by a second-order Taylor series expansion around the equilibrium nuclear geometry, so-called 'mechanical harmonicity':

$$V(\boldsymbol{Q}) = \frac{1}{2}\sum_{k=1}^{3N} \omega_k^2 \cdot Q_k^2, \quad \text{where } \omega_k^2 = \frac{\partial^2 V(\boldsymbol{Q})}{\partial Q_k^2} \qquad (3)$$

Here ω_k is the fundamental angular frequency of the kth vibrational mode, whose motion is described by Q_k. It should be noted that 6 of these angular frequencies (or 5 for linear molecules) correspond to translations and external rotations, which are removed and treated separately. Having established the energies for these transitions, various terms that are needed to construct a Gibbs free energy surface (*e.g.* zero-point energies, thermal corrections and vibrational entropy) can be determined.

Calculation of absorption coefficients requires the use of first order time-dependent perturbation theory.[71] The rate of a transition between initial, $|\nu_i\rangle$, and final quantum states, $|\nu_f\rangle$, denoted $W_{f\leftarrow i}$, can be written:

$$W_{f\leftarrow i} = \frac{1}{\hbar^2}\langle\mathcal{H}_{fi}\rangle^2 \rho_N(\nu_{fi}), \quad \text{where } \langle\mathcal{H}_{fi}\rangle = \langle\nu_f|\mathcal{H}|\nu_i\rangle \qquad (4)$$

Here $\rho_N(\nu_{fi})$ is the density of photon states per frequency range and is the Hamiltonian describing the interaction of light with the system. The molecular systems that are amenable to QM calculations are typically orders of magnitude smaller in dimensions than the wavelengths of non-ionizing radiation (*e.g.* IR and microwaves). The so-called 'long wavelength' approximation assumes that the EMF can be approximated as spatially uniform (while obviously still varying in time), which greatly simplifies the treatment of light/molecule interactions.[71] The magnetic component of radiation, which is small compared with the electric component, is also normally neglected.[71] The resulting simplified Hamiltonian is:

$$\langle H_{fi}\rangle = -\langle\Psi_f|\boldsymbol{\mu}(\boldsymbol{Q})\cdot\mathbb{E}|\Psi_i\rangle \approx -\langle\boldsymbol{\mu}_{fi}\rangle\cdot\mathbb{E}_0, \\ \text{where } \langle\boldsymbol{\mu}_{fi}\rangle = \langle\nu_f|\boldsymbol{\mu}(\boldsymbol{Q})|\nu_i\rangle \qquad (5)$$

Here $\boldsymbol{\mu}_{fi}$ are elements of the resulting transition dipole matrix, which integrates the dipole operator over the normal coordinates, $\boldsymbol{Q}$. This dipole operator is approximated *via* a Taylor series expansion taken around the equilibrium geometry as a function of normal mode coordinates:

$$\boldsymbol{\mu}(\boldsymbol{Q}) = \boldsymbol{\mu}_0 + \sum_k \frac{\partial\boldsymbol{\mu}}{\partial Q_k}\bigg|_0 Q_k, \quad \text{where } \boldsymbol{\mu}_0 = -\frac{\partial V(\mathbb{E})}{\partial\mathbb{E}}\bigg|_{\mathbb{E}=0} \qquad (6)$$

While this expansion is first order in terms of the normal modes that comprise $\boldsymbol{Q}$, dipole moments are themselves first-order response properties of $V(\boldsymbol{Q})$ with respect to an applied EF. Hence the gradient terms used in this expansion are considered

'electronically harmonic', and this expansion does not allow for vibrations involving concurrent electronic excitation. Under these assumptions,[71] the absorption coefficient, $\mathcal{A}_\nu$, is given by:

$$\mathcal{A}_\nu = \frac{1}{4\pi\varepsilon_0}\frac{N_A\pi}{3c}\left(\frac{\partial\boldsymbol{\mu}}{\partial Q_k}\bigg|_0\right)^2 \qquad (7)$$

While the 'double harmonic' approximation is ubiquitous in QM studies, it has well-documented limitations, particularly for describing very low frequency torsional motion.[72–74] These modes are often strongly anharmonic and more accurately considered hindered internal rotations rather than vibrations.[72–74] When considering far-IR/microwave radiation, mechanical anharmonicity is particularly problematic and additional terms in the Taylor series expansion are often used.[72–74]

Explicitly including EFs in electronic structure calculations alters the electronic PES, perturbing both the normal modes Q_k and their corresponding fundamental angular frequencies ω_k. The inclusion of an EF alters the electronic Hamiltonian by introducing an additional term:

$$\mathcal{H}_{EF} = -\boldsymbol{\mu}\cdot\mathbb{E}, \quad \text{where } \boldsymbol{\mu} \equiv -e\sum_i^{N_{\text{electrons}}}\hat{\boldsymbol{r}}_i + e\sum_j^{N_{\text{nuclei}}}Z_j\boldsymbol{R}_j \qquad (8)$$

Here $\boldsymbol{\mu}$ is the dipole moment operator, $\mathbb{E}$ is the EF vector, $\hat{\boldsymbol{r}}_i$ is the position operator for the ith electron, and Z_j and $\boldsymbol{R}_j$ are the atomic number and position (respectively) of the jth nuclei. The effect of these perturbations can be rationalised *via* a Taylor series expansion of the potential, $V(\mathbb{E})$, with respect to the applied field $\mathbb{E}$:

$$V(\mathbb{E}) = V_0 - \boldsymbol{\mu}_0\cdot\mathbb{E} - \frac{1}{2!}\overleftrightarrow{\boldsymbol{\alpha}}\colon\mathbb{E}\mathbb{E} - \frac{1}{3!}\overrightarrow{\boldsymbol{\beta}}\vdots\mathbb{E}\mathbb{E}\mathbb{E} - \cdots \qquad (9)$$

Here V_0 denotes the potential energy at zero field, $\boldsymbol{\mu}_0$ is the permanent dipole moment of the ground-state, $\overleftrightarrow{\boldsymbol{\alpha}}$ is the polarizability tensor and $\overrightarrow{\boldsymbol{\beta}}$ is the first hyperpolarizability. These terms are defined as progressively higher derivatives of the energy with respect to the applied field. Similar evaluations can be performed on oscillating fields to establish analogous frequency dependent properties (*e.g.* dynamic polarizabilities). Most popular QM software packages (*e.g.* Gaussian,[75] QChem,[76] Turbomole[77]) can calculate basic EMF response properties (*e.g.* IR and Raman wavelengths and intensities) and can incorporate static EFs in DFT and wavefunction calculations. More specialised packages, such as TITAN,[78] can generate various types of external EF and quantify intrinsic electric fields within biological systems.

Modelling static and oscillating EFs with *ab initio* molecular dynamics

Rather than using static nuclear configurations and derivative information, *ab initio* molecular dynamics (AIMD) calculates the PES (and forces acting on the nuclei) either in advance, or more commonly, "on the fly" at discrete points at each step of a given trajectory.

The incorporation of EFs in AIMD is discussed extensively in ref. 79, though we provide a brief summary here. For systems

within periodic boundary conditions, a metastable state induced by an external field, $\mathbb{E}$, can be described by the energy functional:

$$E[\{\psi_i\}, \mathbb{E}] = E_0[\{\psi_i\}] - \mathbb{E} \cdot P[\{\psi_i\}] \qquad (10)$$

Here $E_0[\{\psi_i\}]$ is the standard energy functional in the absence of a field and $P[\{\psi_i\}]$ is the polarization along the direction of $\mathbb{E}$. This polarization can be determined from the periodicity of the cell, L, and the elements of the $S[\{\psi_i\}]$ matrix:

$$P[\{\psi_i\}] = -\frac{L}{\pi}\text{Im}(\ln \det S[\{\psi_i\}]),$$
$$\text{where } S_{ij} = \left\langle \psi_i \left| \exp\left(\frac{2\pi i x}{L}\right) \right| \psi_j \right\rangle \qquad (11)$$

The resulting perturbed eigenstates, $|\psi_i^{\mathbb{E}}\rangle$, are given by:

$$|\psi_i^{\mathbb{E}}\rangle = e^{ik_i x}|\mu_i^{(0)}\rangle + \mathbb{E}\sum_{k'} e^{ik'x}|\mu_{k_i \to k'}^{(1)}\rangle + O(\mathbb{E}^2) \qquad (12)$$

This approach can then be used to calculate atomic forces for implementation molecular dynamics schemes.

Classical molecular dynamics

The presence of externally applied EF in classically propagated molecular systems, whether static or time-varying, renders the classical MD simulations as non-equilibrium, thus appropriately referred to as non-equilibrium molecular dynamics or NEMD.

To represent the EF acting on an atomically represented system, the system's Hamiltonian, H, is perturbed by an additional term H_E.

$$H_E(t) = -\boldsymbol{\mu}_{\text{tot}} \cdot \mathbf{E}(t) = -\mu_{\text{tot},z} E(t) \qquad (13)$$

where $\boldsymbol{\mu}_{\text{tot}}$ is the total, collective dipole vector, and E represents the field acting along the z-axis. The method of perturbation depends on whether the system is treated as classical point charges or using electronic-structure approaches, the latter explained in the preceding QM section of the review. Here, we described the formulation of EF in classical molecular mechanics using force fields, where the applied electromagnetic forces are added to the Newton's 2nd law of motion as follows:

$$m_i \boldsymbol{r}_i = \mathbf{f}_i + q_i \mathbf{E}(t) + q_i \boldsymbol{v}_i \times \mathbf{B}(t) \quad \text{where } \mathbf{f}_i = -\nabla_{\boldsymbol{r}_i} V \qquad (14)$$

where the force $\mathbf{f}_i$, is due to the force field determined interactions between all particles (V), $q_i \mathbf{E}$ is the electric field induced force applied to each partial charge i with charge q_i, and $q_i \boldsymbol{v}_i \times \mathbf{B}(t)$ is the Lorentz (magnetic) force acting on individual particle traveling at velocity $\boldsymbol{v}_i$.[80] The electric and magnetic components can be taken to act along the mutually orthogonal x- and y-directions respectively, represented as:

$$\mathbf{E}(t) = \mathbf{E}_{\max}\cos(\omega t)\boldsymbol{k} \quad \text{and} \quad \mathbf{B}(t) = \mathbf{B}_{\max}\cos(\omega t)\boldsymbol{j} \qquad (15)$$

resulting in the plane of polarization being in the x–y coordinate plane, with propagation along the z-axis. The electric- ($\mathbf{E}$) and magnetic- ($\mathbf{B}$) field strengths are related by $\frac{\mathbf{E}(t)}{\mathbf{B}(t)} = c$, where c is the speed of light. Due to the electric-field strength being orders of magnitude greater than that of the magnetic component, common molecular simulation packages such as Gromacs,[81] NAMD[82] and

LAMMPS[83] have only embedded the EF component with continuous and time-variant amplitudes in their algorithms. To the best of our current knowledge, DL-POLY[84] is the only publicly available simulation package through which the magnetic field, albeit separately, can also be applied *via* an external force. There are also several groups which have made in-house modifications to the NAMD and LAMMPS algorithms to incorporate the stand-alone magnetic field forces.[85,86] The first full-representation of the EMF in simulations was achieved by the English group.[87] The code was tested for biologically relevant solvated peptide systems and small differences in peptide conformation between EF and EMF simulations have been observed, however, whether this was due to the additional magnetic force or the finite nature of the simulations remains an open question.[64] Below we review some seminal and most recent (at time of writing) case studies in which molecular modelling of EF/EMF has been employed to better understand the applied field effects on molecules and materials relevant to life systems.

Recent case studies

Water and solutions

Water being one of the most fascinating and important molecules to life plays an important part in many biological and chemical systems. Although water molecule appears quite simple, it possesses an electric dipole and the dynamic behaviour and properties of bulk, surface and interfacial water are controlled by the formation and breaking of orientated hydrogen bonds. As such, the physicochemical properties of liquid water can easily be influenced by EF,[88] and have, therefore, been extensively studied.[34,89–92]

QM studies have mainly focused on quantifying the effect of static EFs on the hydrogen bond structure of molecular water clusters. Kim and co-workers used DFT and wavefunction methodology to investigate the effect of static EFs on the structure, energetics, and transition states of trimer to pentamer water clusters.[93] The authors noted transitions from cyclic to linear water structures when EFs of 3 V nm^{-1} were applied. Pathak and co-workers used similar DFT methodology to investigate the effect of EFs on the structure of water hexamers to octamers.[94] These authors found that increasing EF strength tended to reduce the number of hydrogen bonds within a cluster, with 4 V nm^{-1} fields significantly affecting the relative stability of cluster configurations. Ramalho and co-workers investigated the effect of EFs on larger water clusters $(H_2O)_n$, where n = 2–15, with DFT calculations.[95] These authors noted changes to the number of hydrogen bonds, a reduction in cluster sizes and an increase in the strength of inter-cluster hydrogen bonds.[95] Kreuzer and co-workers used DFT to investigate the formation of whiskers in trimer, tetramer, octamer and decamer water clusters.[96] Interestingly, these authors noted that the HOMO–LUMO gap of the clusters decreased with increasing field strength, approaching zero at the point of structural breakdown of the hydrogen bond networks.[96]

Pathak and co-workers investigated EF responses of larger water clusters, $(H_2O)_n$, where n = 9–20, with DFT calculations.[63]

This journal is © the Owner Societies 2022

Phys. Chem. Chem. Phys., 2022, **24**, 6327–6348 | **6331**

general linear-response régime is in the vicinity of field intensities up to ~0.5–0.7 V nm^{-1}, suggesting that the external field forces and torques should be no more than a few percent of those present intrinsically due to electrostatic fields created by local, intramolecular charge distributions.[34,106] NEMD simulations of liquid water in EF nanosecond pulses were used to evaluate the non-thermal field effects in terms of dipolar response of water molecules.[107] The study was able to show that once the EF was removed, the dipoles relaxed, exhibiting no memory or permanent dipolar alignment, debunking the proposition that water may retain (permanent) "memory"[108] of conditions or EF that it has been subjected to. More recently, the effects of static and high frequency 50, 100 and 200 GHz oscillating fields of 0.5 V nm^{-1} and 1.0 V nm^{-1} rms intensities on liquid water in supercooled and room temperatures (200 to 310 K) were investigated using NEMD simulations and the rigid potential model TIP4P/2005 of water.[109] The authors showed the application of static fields reduced the self-diffusion of liquid water, due to 'dipole-locking', or suppression of rotational motion, whilst diffusivity was enhanced in oscillating fields, especially at high frequencies and outside the supercooled region.

Molecular dynamics simulations have proven useful also in elucidating the dielectric properties, molecular structures, and hydrogen bonding dynamics of glycerol/water mixture exposed to microwave irradiation, due to potential use of glycerol as solvent for nanomaterial synthesis.[110] The study showed that dipole–dipole correlation of glycerol is linked to the field intensity of the microwaves, where the glycerol–glycerol hydrogen bond number and lifetime increased with increasing field intensity up to 1 V nm^{-1}. These results indicated with the assistance of the microwave field, glycerol molecules become more concentrated through higher coordination, which explained the nanomaterial synthesis observations. Externally applied EFs have also been used for their inhibitory effect on electro-coalescence of water-in-oil emulsions. To clarify the mechanism of droplet breakup at the microscopic level, MD simulations have been performed to study the deformation and breakup characteristics of a moving droplet at different field strengths.[111] The results showed that interparticle spacings increased with the growth of the field strength, leading to significantly higher values of the electrostatic potential and van der Waals potential, and hence an increase of the deformation degree. Evidently, there is a critical EF strength, above which droplets undergo a complete coalescence process. An MD study of doubly conducting droplets dissolved in NaCl solution exposed to EF, showed that in presence of EF stronger than the critical field of 0.52 V nm^{-1}, a break-up occurs due to the ion exchange and neutralization in the connecting liquid bridge.[112]

Ionic solutions are particularly interesting models for EF irradiation due to their charged states and the ability of EF to manipulate their associations, diffusion, and structuring. Modelling attempts of ionic liquids have been made using more crude (coarse-grained) approaches,[113] and all-atom simulations using fixed charges which were able to demonstrate the ionic association and transport in electrolyte solution.[114] However, local interactions in a fluctuating charged environment cannot

be easily modelled by static electrostatic parameters, *i.e.*, fixed charges. This is particularly important for highly charged systems such as ionic liquids, enzymes and membranes, thus induced dipoles methods using polarizable force field are needed to model these systems more accurately.[115] Furthermore, the polarized interface between two immiscible liquids is crucial for electro-analytical and ion extraction applications, where an EF is typically used to selectively induce the transfer of ionic species across the interfaces. Computational simulations are useful for modelling such processes. However, due to the long-range nature of the electrostatic interactions and the use of periodic boundary conditions, the use of external EF in MD simulations requires special care. A recent study demonstrated the importance of careful simulation design and setup to accurately model the dielectric response of the materials and that it is possible to obtain the correct EF on both sides of a liquid–liquid interface when using standard 3D Ewald summation methods.[116]

One of the disadvantages of using the constant force/field method for modelling the responses to externally applied fields is its inability to properly capture the propagation of the electric field across the system under study. In experimental setting, the electric field emanates from the anode, penetrating through the sample toward the cathode. The electric field is substantially weakened (shielding) as it penetrates through a liquid sample, due to the high relative dielectric permittivity of water. This is important consideration since physical properties such as mobility exhibit different behaviour at the liquid–vapor interface in comparison to the bulk, where at the interface the coordination number of the hydrated ions and the local field are different from the bulk.[117]

The Constant Electrode Potential Method (CPM)[118] enables an external electric field to be applied on a system, accounting for the shielding effects by water. A recent study employed the CPM method to investigate the effects of an external electric field on the surface tension of water and to compare that to the conventional (constant force) method, in addition to computing the interfacial mobilities of Na$^+$ and Cl$^-$ ions at a liquid–vapor interface.[119] The CPM method was able to predict a weaker variation in the surface tension in comparison to that of the conventional method, with the maximum reported difference being 36% of the surface tension value.

Although the above QM and classical MD studies do not always directly refer to biological systems, the behaviour of water molecules, clusters, droplets and, especially, physiologically relevant salt solutions is crucial for understanding the effects of EMFs on larger scale aqueous biomolecular assemblies.

Proton transfer in DNA

Deoxyribonucleic acid (DNA) stores biological information that is essential for the development, normal functioning, and reproduction of all known organisms. Over 50 years ago, Lowdin proposed that proton transfer reactions between base-pairs could alter DNA's underlying hydrogen bond structure and introduce mutations, the so called 'rare tautomer' hypothesis of spontaneous mutagenesis.[120,121] This tautomerisation is thought to be the potential origin of spontaneous DNA errors

This journal is © the Owner Societies 2022

Phys. Chem. Chem. Phys., 2022, **24**, 6327–6348 | **6333**

by introducing point mutations during replication (*e.g.* GC → AT, see Fig. 3). While the thermodynamic stability of canonical base-pairs minimises the mutagenic potential of these rare tautomers, it is thought that environmental agents could potentially enhance these underlying proton transfer reactions.[122] For instance, pairing of unnatural nucleobases, ionizing radiation and intercalating agents have been found to influence the stability of these tautomers.[123–125] Guanine–cytosine (G:C) base-pairs are known to be more susceptible to tautomeric induced mutations, with adenine–thymine (A:T) pairs showing greater resistance.[126–128] As different tautomers can possess markedly different electrostatic properties (*i.e.* partial charge distributions, dipole moments), EFs are likely to alter both their stabilities and rate of interconversion. Relatively intense pulsed EFs ($10^{-3} - 10^{-2}$ V nm^{-1}) have been investigated for medical applications, specifically delivery of non-permeable drugs and gene therapy (*via* electroporation).[42,129–132] Indeed, 0.06 V nm^{-1} picosecond pulsed EFs have been investigated experimentally for the treatment of tumours.[133] Thus, the potential impact of such fields on the structure and stability of DNA is of significant interest.

Computational interest in potential EF effects on double stranded DNA arose following a seminal QM study by Matta and Arabi, which found that external EFs influenced the equilibrium structure and hydrogen transfer kinetics of the formic acid dimer.[134] Following a detailed QM study of the effect of Mg^{2+} cations on Lowdin tautomerisation,[135] Jacquemin and Cerón-Carrasco investigated the effect of external EFs on a model G:C base-pair with QM calculations.[60] These authors found that strong EFs can significantly influence the rate coefficients and mechanism of proton transfer that lead to rare G:C tautomers. EFs on the order of 0.5–4 V nm^{-1} lowered the barrier leading to the G*:C* tautomer by 20–55 kJ mol^{-1}, though stabilisation of the G*:C* tautomer itself was more minor (≤ 10 kJ mol^{-1}). Consequently, the G*:C* tautomer had a shallow energy profile in the presence of EFs, with reversion to the canonical base-pairs

being essentially barrierless. Moreover, the estimated equilibrium constant for G*:C* tautomer formation across all EF strengths was small ($\sim 10^{-6}$–10^{-8}). In contrast, at fields of 3–5 V nm^{-1}, the G$^-$:C$^+$ zwitterion was found to be comparably stable to (or even more stable than) canonical G:C base-pairs. Further to this, in the presence of these fields, G$^-$:C$^+$ zwitterions were well-defined minima, with substantial equilibrium constants of formation ($\sim 10^{-1}$–10^{5}) and significant barriers to reversion. The authors concluded that in the presence of EFs, only G$^-$:C$^+$ zwitterions fit the necessary kinetic criteria to be considered a viable route to mutagenesis (see ref. 127). Following this initial study, Jacquemin and Cerón-Carrasco applied a hybrid ONIOM style (QM/QM′) approach to investigate a more realistic d(5′-GGG-3′):d(3′-CCC-5′) DNA fragment and account for stacking of adjacent nucleobases.[61] These calculations broadly supported their earlier conclusions, though EFs ≤ 1 V nm^{-1} had no discernible effect on the barrier for G*:C* formation. However, at fields ≥ 2 V nm^{-1}, the double hydrogen transfer to form G*:C* was barrierless, with these rare tautomers possessing very shallow potential energy profiles. At field intensities ≥ 4 V nm^{-1}, the G$^-$:C$^+$ zwitterion was again found to be more stable than canonical G:C base-pairs and met the necessary requirements to be considered a potential source of mutagenesis. To ascertain if these EFs would influence the tertiary structure of DNA, Jacquemin and Cerón–Carrasco used classical MD to investigate the dynamic response of a dodecamer duplex dG12:dC12.[62] These authors found that continuous application of intense EFs (≥ 3 V nm^{-1}) causes unwinding of double stranded DNA within 10 picoseconds.[62] However, these authors proposed that external EFs around 3 V nm^{-1} applied in 5 picosecond pulses could potentially induce selective mutation (*via* the G$^-$:C$^+$ zwitterion) while also limiting changes to the tertiary structure of DNA.[62]

More recently, Matta and Arabi used QM methodology to verify that A:T base-pairs were considerably less susceptible to tautomeric mutation, even in the presence of strong external
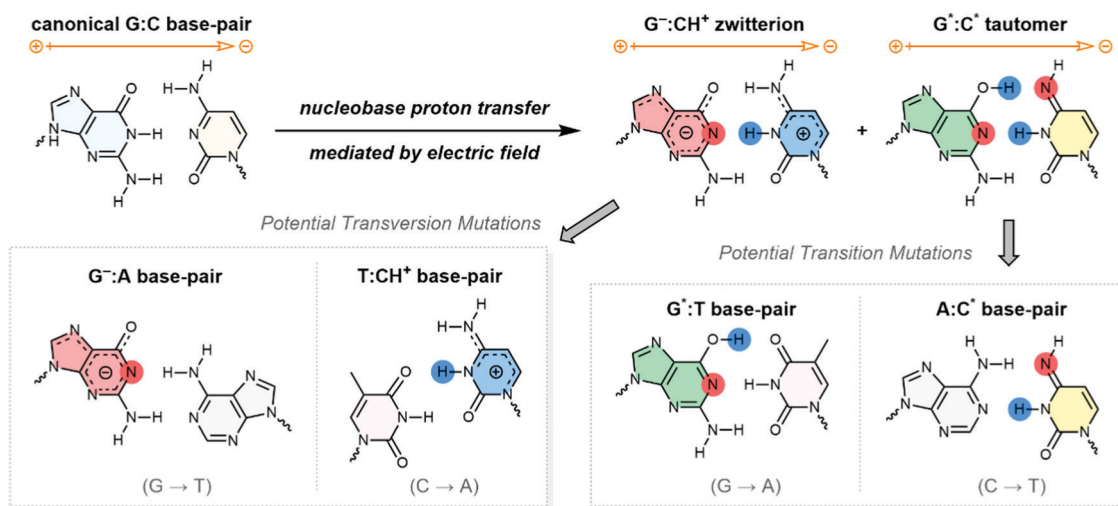
Fig. 3 The chemical structure of a canonical G:C base-pair, G$^-$:CH$^+$ (iminium/azanide) zwitterion and G*:C* (enol/imino) rare tautomer. The direction of the EF required to induce these proton transfers is indicated by an orange arrow. Hypothetical point mutations that could arise from these non-canonical base-pairs are given in parenthesis. Solid red circles indicate the deprotonated heteroatom, while solid blue circles indicate the transferring proton.

6334 | *Phys. Chem. Chem. Phys.*, 2022, **24**, 6327–6348

This journal is © the Owner Societies 2022

EFs (up to 5 V nm^{-1}).[136] Matta and Arabi also used QM methodology to investigate EF effects on the formation of the G*:C* tautomer, accounting for quantum tunnelling effects.[137] These authors thoroughly characterised the effect of EFs on the order of 1 V nm^{-1} on the kinetics and thermodynamics of G*:C* tautomerisation. Very recently, Arabi and co-workers used QM/MM and classical MD simulations to study the effects of EF ranging from 10^{-5}–1 V nm^{-1} on a dodecamer DNA model.[138] Consistent with earlier studies, the authors noted the application of large EFs ($\sim$1 V nm^{-1}) increased the thermo-dynamic population of G*:C* tautomers by up to 1 order of magnitude.[138] However, in contrast to the previous studies of Cerón-Carrasco and Jacquemin,[60–62] Arabi and co-workers also noted the formation of the G$^-$:C$^+$ zwitterion at lower EF strengths ($\sim$1 V nm^{-1}).[138] However, we should note that these studies not only employed different methodologies (e.g. different sized QM models and density functionals) but also investigated a differing configuration of stacking nucleobases. Ultimately, Arabi et al. concluded that at EFs of $\leq$1 V nm^{-1}, both the G*:C* tautomer and the G$^-$:C$^+$ zwitterion were too transient to contribute towards mutations, as their lifetimes were on the order of picoseconds compared to the nanosecond timescale for DNA opening during replication.[138]

While double helices are the most common tertiary structures adopted by DNA, other structural motifs have also been identi-fied at lower concentrations. G-quadruplexes are helical G-tetrads formed from DNA sequences rich in G-bases (see Fig. 4). These tertiary structures are much rarer than canonical double helices but are thought to play an important role in cellular function and replication.[139] Capitalising on insights from their previous studies, Jacquemin and Cerón-Carrasco used QM/MM methodology to study the effect of EFs on a model trimeric G-quadruplex (see Fig. 4, left).[140] As with their previous studies, G-quadruplexes were found to be susceptible to tauto-merisation when external EF around 4 V nm^{-1} were applied.[140] The most favourable rare tautomer identified was an oxonium/azanide zwitterion (Fig. 4b), with the iminium/azanide zwitterion (Fig. 4c) and quadruple enol/pyrimidine tautomer (Fig. 4d) found to be significantly less stable (regardless of field intensity). While the quadruple enol/pyrimidine tautomer was found to be a stable minimum even in the absence of applied EF, neither zwitterionic structure was stable when the applied EF was less than 4 V nm^{-1}. This study concluded that the sensitivity of G-tetrads (within G-quadruplexes) to external EFs is comparable to that of G:C base-pairs (within double stranded DNA), despite the differences in secondary and tertiary structure.
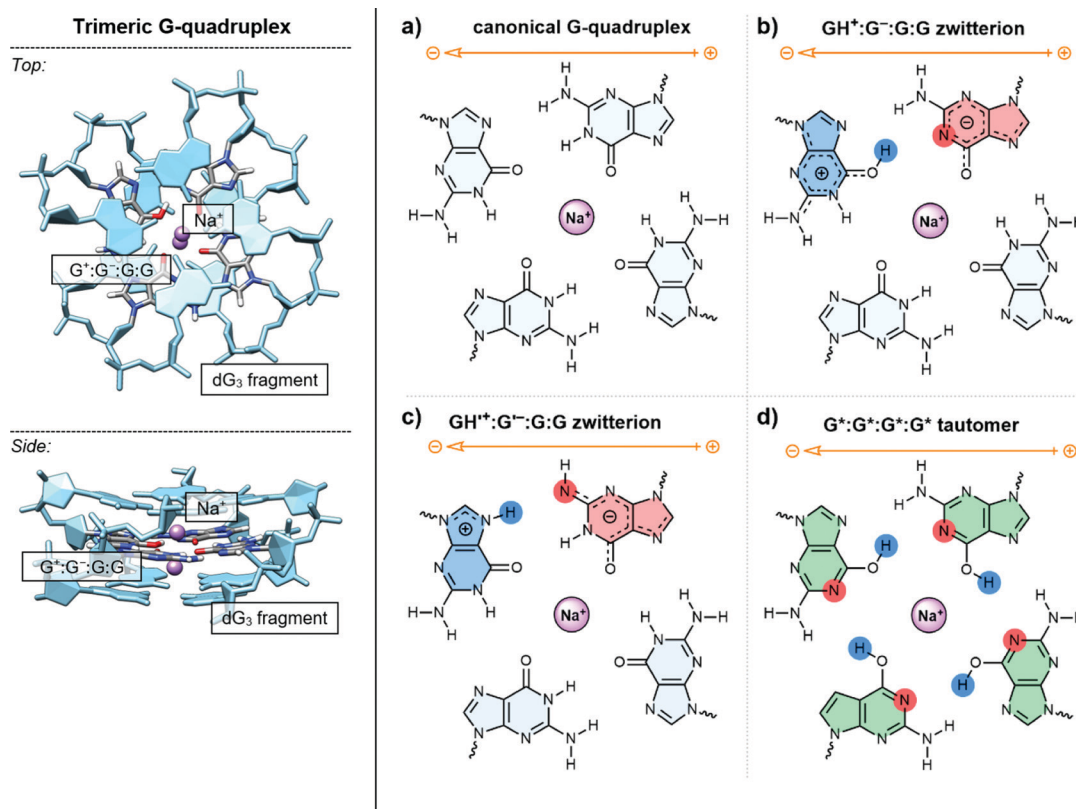
Fig. 4 Left: The trimeric G-quadruplex investigated by Jacquemin and Cerón-Carrasco, with the central quadruplex (depicted atomistically) shown in its G$^+$:G$^-$:G:G (oxonium/azanide) zwitterion form. Optimised structure taken from ref. 140. Right: Chemical structures of a canonical G-quadruplex, G$^+$:G$^-$:G:G (oxonium/azanide) and GH$'^+$:G$'^-$:G:G (iminium/azanide) zwitterion, and a G*:G*:G*:G* (quadruple enol/pyrimidine) rare tautomer. The direction of the EF required to induce these proton transfers is indicated by an orange arrow. Solid red circles indicate the deprotonated heteroatom, while solid blue circles indicate the transferring proton.

Intercalated-motifs (i-motifs) are tetrameric DNA structures that consist of two parallel duplexes combined in an anti-parallel manner (see Fig. 5). They are typically formed in C-rich sequences and thus are often encountered on complementary strands of G-rich (G-quadruplex forming) sequences. While the stability of i-motifs is dependent on their environment (*e.g.* pH),[141] it has been postulated that they play a role in gene expression as well as DNA replication and repair.[142] Recently, Jacquemin and Cerón-Carrasco used QM calculations to investigate the effects of external EFs on a hemi-protonated-C:C dimer (CH$^+$:C), which is the central moiety of the i-motif (see Fig. 5, left).[143] Intriguingly, these calculations indicated that this dimer is significantly affected by weaker EFs ($\sim$0.5 V nm^{-1}), which block normal proton exchange between the C nucleobases (see Fig. 5, right).[143] In the absence of external EF, the CH$^+$:C and C:CH$^+$ base-pairs are degenerate with the central proton undergoing rapid exchange ($k_{\text{trans}} \sim 10^{11}$ s^{-1}).[143] However, in the presence of a 0.5–2.0 V nm^{-1} EF, the C:CH$^+$ configuration (relative to the applied EF) is 6–27 kJ mol^{-1} more stable than its CH$^+$:C counterpart.[143] As this exchange process plays a fundamental role in delocalising the cationic character of the CH$^+$:C base-pairs, it mitigates the risk of side-reactions with the surrounding molecules (*e.g.* oxidation by water).[143] By blocking this exchange process, external EFs effectively localise the cationic character of i-motifs onto a single C base, which may increase the probability of deleterious reactions with the surrounding media.[143]

Fig. 5 Left: A prototypical i-motif, with the two central hemi-protonated base-pairs (CH$^+$:C) depicted atomistically. Taken from ref. 141 (PDB ID: 5OGA). (right) Chemical structures of the protonated CH$^+$:C base-pair and the functionally equivalent C:CH$^+$ base-pair, which is degenerate in the absence of an applied EF. The direction of the EF required to block this proton transfer is indicated by the orange arrow. Red circles indicate the deprotonated heteroatom, while blue circles indicate the transferring proton.

Protein structure and dynamics

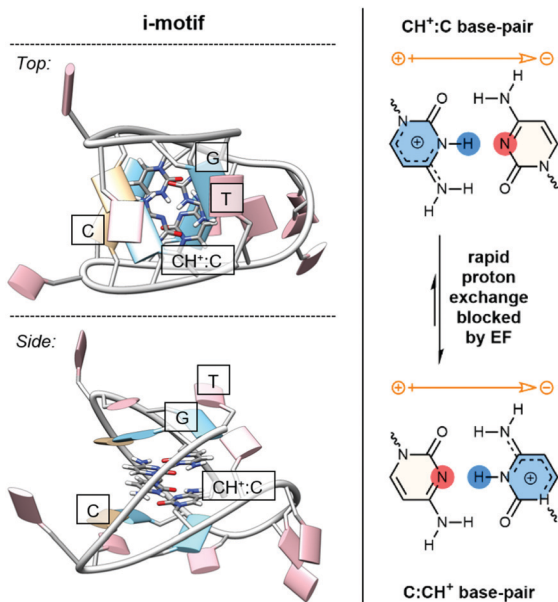Over the last decades there has been tremendous interest for an improved understanding of the effects of EFs on protein structure and dynamics using experimental[3,47] and computational techniques.[144,145] The thermal effects of EF irradiation have been well studied and are easier for interpretation mostly due to the expected inherent denaturation of proteins at increased temperatures.[146–148] The mechanisms of non-thermal EF effects, however, remain poorly understood. This is mostly due to the interconnection of specific EF frequencies and strengths capable of exciting certain vibrational modes of proteins and peptides, causing (sometimes irreversible) structural changes which can affect their structure, behaviour and function.

QM-based studies of EF effects on standard proteins are usually prohibitively expensive, so work has generally focused on prototypical model fragments of relevance to protein structure (*e.g.* salt bridges) and small peptides. Most of these studies have focused on the computational prediction of Vibrational Circular Dichroism (VCD) and Raman Optical Activity (ROA) spectra, which can be used to characterise the structure of peptides. For instance, Jalkanen and co-workers studied the spectroscopic properties, including in the mid- and far-IR regions, of L-alanine in the gas-phase and in non-polar solvents with DFT.[149] Similarly, Suhai and co-workers used DFT to examine the spectroscopic properties of various amino acids and small peptides.[150] Other studies have used DFT to predict spectroscopic behaviour of, for instance, model 3$_{10}$- and α-helices,[151] β-hairpin structures[152] and γ-turns.[153] Various other small biomolecules and fragments have also been examined with QM-based approaches.[154–157] However, as the application of VCD and ROA spectroscopy for peptide structural characterisation was recently reviewed by Keiderling,[158] we focus here on studies that explicitly consider the structural effects of relatively intense EFs. Dudev and co-workers examined the effect of static EFs on the secondary structure of a range of model helical peptides.[45] These authors found that application of intense external fields (>2.5 V nm^{-1}) along the axis of the helix resulted in the loss of helical structure and formation of unusual cyclic/ring peptide conformations.[45] Dudev and co-workers also examined the impact of external EFs on a model salt-bridge peptide, finding minimal disruption of the underling Lys-Asp pair at the field strengths and orientations studied.[45] While these authors noted that these EF-induced perturbations of secondary structure were reversible,[45] we should emphasise the peptides were considered in isolation. Bhattacharyya and co-workers studied EF effects on a Lys-Asp pair as a model salt-bridge, noting some changes in electrostatic properties and interaction energies under intense fields.[159] While intense EF can induce spontaneous proton transfer in ion-pairs, generally fields >2.5 V nm^{-1} are required.[160]

Over the last few decades, numerous QM and QM/MM studies have uncovered the role of internal (or intrinsic) electrostatic interactions in modulating enzyme activity. Enzymes have evolved highly tailored structures that specifically orientate charged and polar residues around bound substrates, creating highly complex and anisotropic electrostatic environments in their active sites. While many QM/MM studies have investigated

electrostatic catalysis in enzymes, significant emphasis is usually placed on quantifying and replicating the intrinsic electrostatic environment of the active site. However, a few illustrative studies have examined the effects of simple external EFs on active site catalysis. For instance, pioneering work by Shaik and co-workers examined competing C–H hydroxylation and epoxidation mediated by heme species in the presence of external EFs.[161] The heme species possessed no selectivity in the absence of an external EF, however application of EFs on the order of 5 V nm^{-1} provided high selectivity for each pathway (depending on applied field orientation).[161] Another elegant QM/MM study by Shaik and co-workers examined the effect of external EFs on the catalytic cycle of cytochrome P450.[162] External fields influenced the initial gating cycle, rate-determining step, O_2 uptake, resting state geometry and spin-state ordering of various active species, with particularly large effects noted perpendicular to the porphyrin plane.[162] Timerghazin and Talipov used DFT to study external EF effects on the properties and reactivity of *S*-nitrosothiols, which are ubiquitous carriers of nitric oxide.[163] They noted that barriers for *trans-S*-nitrosation and *S*-thiolation were highly dependent on EF strengths and orientations, with the electrostatic environment controlling the resulting kinetic selectivity.[163] Dudev and co-workers have also investigated the impact of external EFs on binding selectivity of metalloproteins.[164]

Classical MD simulations have shown to be particularly useful in elucidating the dynamics and conformational changes in peptides and protein in the presence of static, time-varying and pulsed EF with varying characteristics. The complementarity of quantum and classical theory simulation methods was recently demonstrated in the possibility to orient gas-phase proteins such as ubiquitin using time-dependent EF.[165] The *ab initio* simulations were used to estimate the field strength required to break protein bonds, with 45 V nm^{-1} as a breaking point value while the MD simulations showed the minimal field strength required for orientation within 10 ns to be on the order of 0.5 V nm^{-1}. Although high fields can be destructive for proteins, the structures in these simulations were preserved until orientation was achieved regardless of field strength, a principle the authors denoted as "orientation before destruction." Following this study, Sinelnikova *et al.* identified the unfolding pathways of ubiquitin, induced by experimentally achievable external electric fields. Their simulations showed that strong EF in conjunction with short-pulsed X-ray sources such as free-electron lasers provide a means for imaging dynamics of gas-phase proteins at high spatial and temporal resolution.[58]

In an all-atom explicit solvent simulations, Budi *et al.* found that both static and oscillating fields influence the insulin chain-B conformation, with the latter being more disruptive to the structure compared to static fields of similar effective strength.[166] In a follow up studies, the effects of oscillating fields of different frequencies was explored for the isolated chain B[167] and complete insulin monomer.[166] Their results showed the application of lower-frequency 1.225 GHz oscillating fields allowed the peptide dipole moment to consistently

respond to the applied field, *via* the modulation of conformational changes within each field direction, compared to the peptide dis-orienting high frequency of 4.9 GHz field. Studies of pectin methylesterase (PME) showed EF exert non-thermal effects on both local and global protein structure.[168] The 1 μs simulations demonstrated significant shrinkage of the catalytic domain and shortening of enzyme–water hydrogen bond lifetime due to field strengths of equivalent energy input of 5×10^{-6} V nm^{-1} experimental EF. Unwinding of the helical segments, altered intra- and intermolecular hydrogen bond patterns, and increased hydration were also caused by the 5×10^{-6} V nm^{-1} EF. This and other similar studies[1,87] have shown that catalytic activity of enzymes can be enhanced or inhibited by manipulating the electric field strength, frequency, and treatment temperature. Furthermore, short (<100 ns) and intense (>0.0007 V nm^{-1}) EMF pulses have also been shown capable of modulating protein structure and function.[2,169]

More recently, the potential effects of EF on the structure and function of the spike protein found on the SARS-CoV-2 virus, responsible for the COVID-19 pandemic was explored using MD simulations (Fig. 6).[170] The sub-microsecond simulations showed that on a EFs of much lower intensities (10^{-4} – 10^{-2} V nm^{-1}) can cause significant damage to the tertiary and secondary structure of the spike protein, affecting its interaction with the virus human host cell membrane receptor angiotensin-converting-enzyme (ACE2) and potentially rendering SARS-CoV-2 less infectious.

Changes to the native or physiological/functional conformations can lead to misfolding and the formation of pathogenic structures of proteins, which can self-assemble into insoluble aggregates, known as amyloid fibrils. These fibrous deposits have been linked to systemic and neuro-debilitating diseases, such as atherosclerosis, Alzheimer's, Parkinson's, and others.[171,172] Curiously, on the other hand, experimental studies have suggested that EMFs may be used as a therapeutic tool for the breakdown of fibrils implicated in Alzheimer's disease.[15,57] Therefore, an improved understanding of the effects of radiofrequency radiation on biomolecules and their implications in disease processes at the molecular level has been the goal of several research groups.[7,55,144,173] The multivalent interactions during folding/misfolding and self-assembly, combined with the associated complexities of proteins due to their variability in size and sequence require a systematic simulation approach to reproduce and explain the associated adverse or beneficial effects of EF. For example, a series of explicit solvent MD simulations were applied to investigate the effects of EMFs on the amyloidogenic apoC-II(60–70) peptide, implicated in fibril formation by the ApoC-II lipid transport protein associated with heart disease.[56] The simulations of varied electric field strength from 0.7 V nm^{-1} to a relatively low intensity field of 0.0007 V nm^{-1}[64] showed that field strengths lower than 0.004 V nm^{-1} had no tangible effects on the peptide conformation. The intermediate field-strength range (0.04–0.004 V nm^{-1}) caused a significant increase in peptide dynamics, which resulted in an increased population of structures with fibril-inhibiting characteristics, such as the separated N- and C-termini and colocation of the aromatic residues at the same peptide face. The high strength
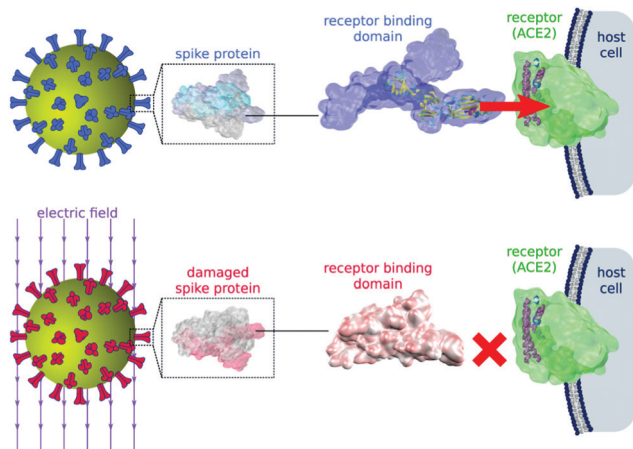
This journal is © the Owner Societies 2022

Phys. Chem. Chem. Phys., 2022, **24**, 6327–6348 | **6337**

Fig. 6 Virus entry into the cell is mediated by the recognition between the spike glycoprotein (S protein) present in the virus envelope and the host cell membrane receptor ACE2. The binding between the S protein and ACE2 can be altered when external electric fields induce drastic conformational changes and damage in the S protein.[170]

(>0.04 V nm^{-1}) field simulations, apoC-II(60–70) experienced peptide dipole alignment along the applied field direction, which resulted in elongated structures and disrupted the inherent β-hairpin conformation known to be the intermediate state for fibril formation. In a follow up study, the role of frequency in the radiofrequency (1.0 and 2.5 GHz) and higher frequency (5.0 GHz) ranges was investigated.[174] The study showed that the EM field induced peptide conformations dependent on the field frequency and strength. At the high field strength (0.7 V nm$_{rms}^{-1}$), the peptide explored a wider conformational space as the frequency increased from 1.0 to 5.0 GHz. At the intermediate strength fields (0.07–0.0385 V nm$_{rms}^{-1}$), the frequencies of 1.0 and 2.5 GHz resulted in the peptide being trapped in specific conformations, with 1.0 GHz enabling both fibril-forming and fibril-inhibiting conformations, while 2.5 GHz led to formation of mostly fibril-competent conformations. In contrast, the 5.0 GHz frequency caused increased peptide dynamics and more extended conformations with fibril-enabling aromatic side-chain arrangement akin to the structures formed under ambient conditions. All the simulated frequencies at low strength fields (0.007–0.0007 V nm$_{rms}^{-1}$) resulted in the formation of amyloid-competent hairpin conformations alike those formed under the weak static EF and ambient conditions. Similarly, Derreumaux et al. used MD simulations to explore the impact of transmembrane EF (0.02 V nm^{-1}) on an Alzheimer's implicated Aβ peptide model in solution[175] and at the membrane.[48] The study demonstrated rupture of the Aβ supramolecular assembly caused by protein chains rearrangement and increase of dipole moment.[173] These results suggest that specific ranges of EMF parameters produce peptide/protein conformations unfavourable for formation of amyloid fibrils, a phenomenon that can be exploited in treatment and prevention of amyloid diseases. Alternatively, EMF parameters can be selected to modulate the formation of well-ordered peptide/protein assemblies as a rational design strategy for engineering biocompatible materials.

Membranes

Intense static or pulsed electric fields are known to act at the cell membrane level and are already being exploited in biomedical and biotechnological applications.[16,176] Biological cell membranes have been found to become permeable (electropermeabilisation), either reversibly (at low field strengths), or irreversibly (at higher field strengths). This phenomenon has been found useful in extraction of bioactive compounds, breakdown of cellulosic materials, and inactivation of microorganisms. It is well known that EFs can also create pores in membranes (electroporation) which enable transfer of ions, genetic materials and other small solutes across the membrane. The mechanisms of electropermeabilisation and electroporation remain elusive and difficult to visualise experimentally, thus molecular simulations have become very useful in the study of these processes.[177]

Computational approaches have shed light on the local perturbations at the membrane interface upon exposure to external stresses, such as those of applied EF. One such study showed that when transmembrane voltage is higher than a certain threshold, hydrophilic pores were formed and stabilised by the membrane lipid headgroups within the nanosecond time scale.[178] The mechanisms responsible for membrane permeabilisation, and structural or dynamic changes imparted on biomolecules by high-frequency (18 GHz) electromagnetic irradiation were recently explored using experimental and computational techniques.[59] This work suggested that the EMF-induced oscillations, i.e., vibrations and reorientation of water molecules (dipoles) may be able to induce liposome bilayer permeability without affecting their integrity, thus presenting opportunities in applications of EMF for transporting therapeutics to and across live cell membranes. Specifically, extremely high strength fields (0.21 V nm$_{rms}^{-1}$) were able to cause an increase in the interfacial water dynamics characterised by water dipole realignments, in the all-atom POPC membrane modelled by classical MD simulations for 200 ns (Fig. 7). At the lower field strengths (<0.21 V nm$_{rms}^{-1}$), high frequency EMF induced changes of the water hydrogen bond network, which may contribute to the mechanisms that facilitate membrane permeabilisation within a longer timeframe.

In typical electroporation treatments, EF higher than the membrane breakdown potential is usually applied so that transient membrane defects can be formed in advance before delivering extracellular materials. Shimitzu et al. used coarse-grained MD simulations to study the permeation of a cationic gold nanoparticle (AuNP) across zwitterionic and negatively charged phospholipid bilayers under an EF.[179] When an EF that is equal to the membrane breakdown potential (intensity) was applied, a typical NP delivery by electroporation was shown whereby the cationic AuNP directly permeated across a lipid bilayer without membrane wrapping of the AuNP, while a persistent transmembrane pore was formed (Fig. 8). However, when a specific range of the EF that is lower than the membrane breakdown intensity was applied, a unique permeation pathway was exhibited where the generated transmembrane pore immediately resealed after the direct permeation of AuNP. The affinity of the NP for the membrane surface was found to be a key for the self-resealing of the pore.
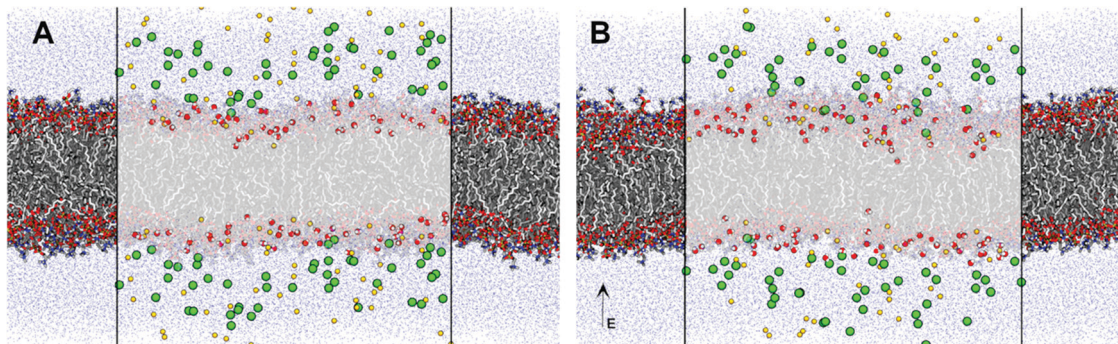
Fig. 7   Exemplar MD simulated molecular representation of the POPC membrane (shown in licorice) exposed to (A) ambient and (B) 0.21 V nm$_{rms}^{-1}$ high frequency electric fields, demonstrating the deeper penetration of water during irradiation (the EF direction shown by arrow). Water molecules within 1.6 Å of the membrane are shown in vdW surface representation, and all other water molecules as blue points. The sodium and chloride ions are shown as their vdW surfaces coloured yellow and green respectively.[59]

More recently, the same group explored the translocation mechanisms of negatively charged NP across negatively charged membrane using coarse-grained MD simulations.[180] The study showed that while it would generally be electrostatically impossible under ambient conditions, in their model the anionic NPs were able to translocate across a negatively charged membrane *via* a non-disruptive pathway under a weak EF due to an ionic charge imbalance. This is a theoretical demonstration that negatively charged NP can, in fact, be delivered into a cell by combining applied EF with membrane hyperpolarization/depolarization induced by an external stimulus.[181]

Cell-penetrating peptides have a wide biomedical appeal due to their "designability", low cytotoxicity and ability to penetrate membranes, the latter being possible mostly at high peptide concentrations or by being attached to various nano-carriers.[182,183] External stimuli, such as EF can also be utilised to enhance cell-permeation by CPPs in controllable ways.[184] The processes of single polyarginine (R8) peptide penetration through planar and vesicle membranes under an external electric field were simulated *via* coarse-grained MD simulations.[185] The study showed that the EF strength and membrane curvature affect the penetration rate of the charged peptide across the membrane. The peptide penetration time across the planar and curved membranes decreased with increasing amplitude of the EF applied. The membrane curvature allowed for faster translocation of the peptide compared to planar membrane due to the increased surface tension and larger area per lipid for vesicle membranes.

Bionanomaterials

The immense potential of nanomaterials for biomedical and industrial applications can be realised *via* the ability to control the rotation, translation and cooperativity of intra- and inter-molecular dynamics, the key factors for the design and development of stimuli-responsive "smart" materials or artificial molecular machines.[186] Electric fields have been employed to control nanoscale robotic arms,[187] molecular gates,[188] and induce structural changes in metal–organic frameworks (MOFs) to modulate the materials electric properties,[189] and tune the porosity of MOFs for single-gas membrane permeability.[190] MD simulations were employed to investigate intense (0.1 V nm^{-1}) nanosecond-scale EF effects on the structure and dipolar properties of the kinesin nanomotor.[191] Kinesin is a biological molecular
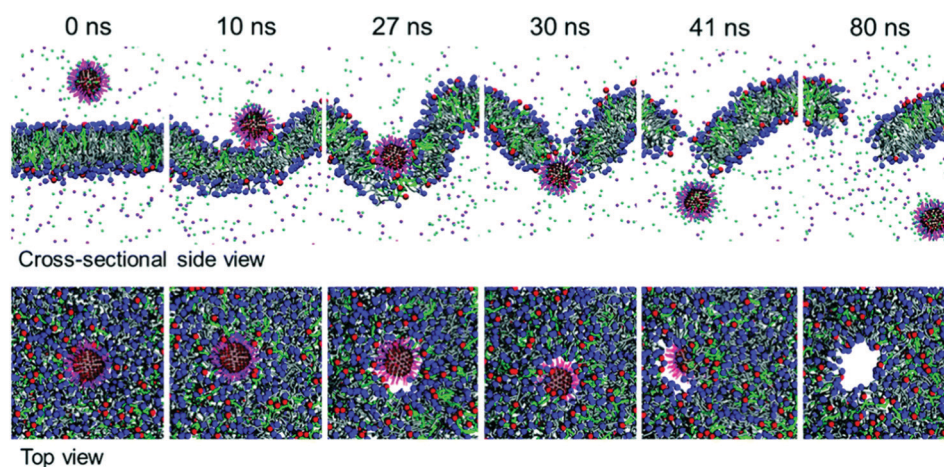

Fig. 8   Cross-sectional side view and top view during nanoparticle permeation of DPPC/DPPG membrane model under externally applied field (V^{*} = 1.0).[179]

nanomotor which converts chemical energy into mechanical work. The study showed that the function of biological molecular motors can be altered by external irradiation, providing means for the development of novel electromagnetic methods for nanobiotechnology.

The ability of EF to modulate the dipolar orientation and thus the structure of molecules provides an opportunity to control how molecules bind to different materials. The effect of static EF on the adsorption mechanisms of single amino acids on the bare/unprotected Au(111) surface was explored using MD and free energy calculations with the purposely developed Golp-CHARMM forcefield which represents the image charge interactions important for modelling metallic surfaces.[192] The study showed that adsorption of positively charged AAs (arginine, histidine, and lysine) is more affected by the EF than that of negatively charged (aspartic and glutamic acids) and charge-neutral AAs (alanine, glycine, tryptophan, and asparagine). The difference arises from the role of a charged side chain in the molecule's adsorption on the gold surface. The adsorption *via* a deprotonated carboxyl group was observed to be less favourable and was facilitated by hydrogen bonding with the adsorbed water, while the positive amines directly interacted with surface gold atoms. This explained the relatively weaker adsorption of negatively charged AAs and their smaller scale response to the EF due to solvent-induced electrostatic screening. These results provide insights into the molecular arrangement at the biointerfaces with gold exposed to EFs, which can be exploited for more controlled design of bionanomaterials.

MD simulations were used to investigate the ability of EFs to modulate the mechanical properties of polyelectrolytes and to understand the governing mechanisms.[193] Mechanical property modulation by EF was found to be sensitive to the charge distribution—charges must be tightly attached to the polymer backbone, and responsivity is greater if a single backbone contains both positive and negative charges. The dominant mechanisms are reorientation and stretching of the polymer chains, which also elongate the ionic clusters to maintain strong electrostatic interactions throughout deformation. These insights are critical for future experimental realisation of polymers with EF regulated mechanical properties.

Summary and future perspectives

The case studies summarised demonstrate the need for more holistic multiscale computational approaches to properly investigate the enthalpic and entropic effects of applied electric fields on molecular systems in realistic biologically relevant environment, from charge transfers and bond breaking/formations to dynamical phenomena such as protein conformational changes and lipid membrane lability. While most QM studies published on external EFs have examined fields that are uniform and static, increasingly powerful computation resources (and improvement software efficiency) should greatly improve the feasibility of modelling biomolecular systems under dynamic EFs and EMFs. Moreover, the development of specialised software packages specifically tailored for QM-based EF and EMF calculations will also help facilitate new research in this area.

In the classical realm, with the computational power and infrastructure dramatically increased over the last decades, it is now feasible for EMF effects to be modelled on long(er) time and length scales, thus enabling observation and quantitative characterisation of tangible molecular level effects of much lower field intensities than previously possible. Furthermore, the longer simulation times ensure a significant count of EF cycles can be implemented for lower frequency fields to collect statistics sufficient for reliable characterisation of biomolecular dynamics and response kinetics at the physiologically relevant timeframes.

The ongoing development of enhanced sampling methods can address the large separation in time scales between molecular dynamics simulations (usually microseconds or shorter) and the time scales of biological processes (often orders of magnitude longer). However, enhanced sampling techniques such as the family suite of metadynamics methods enable improved exploration of the free energy landscape where time-dependent changes such as those induced by oscillating electric fields are not of essence. Therefore, the spontaneous time evolution of biologically relevant systems under the external EMFs may be necessary to observe structural and dynamic molecular changes for reporting any evidence-based conclusions about the effects of radiation on the biological matter.

While the direct comparisons of the EMF induced perturbations to the electronic and atom-resolved structure of the biomolecules and their assemblies with experiments may not be possible, largely due to the lag of the experimental techniques, it is essential to test the computational methodologies for their ability to reproduce the ambient behaviour of biological molecules and previously experimentally identified changes for future benchmarking of any external EMF effects. Further to this, since in biologically relevant systems EMFs can perturb charged and polarisable particles in polarisable environment, it is important to consider polarisation effects and/or electronic degrees of freedom in the theoretical models, which are not yet accounted for by most common forcefields employed with classical MD simulations. There is, therefore, a need to further explore polarisable forcefields developed for and increasingly applied to polarisable systems (*e.g.* ion channels), including AMOEBA[194] and Drude forcefields.[195–197] albeit they come with their own challenges and limitations.[198]

Overall, with the growing interest in applications of the EMF based technologies in contemporary life, from mobile telecommunication to medical treatments and defence technologies, it is clear that predictive capabilities offered by the multiscale simulations for evaluating effects of the external field parameters on a comprehensive range of molecular responses within the biological matter or biomedical materials and technologies are now more crucial than ever. Most importantly, the theoretical simulations continue to provide insights not accessible through experimental observation and, therefore, represent an indispensable

6340 | *Phys. Chem. Chem. Phys.,* 2022, **24**, 6327–6348

This journal is © the Owner Societies 2022

tool for furthering our understanding of the electromagnetic bioeffects in life tissues and novel biomedical and engineering devices.

Conflicts of interest

There are no conflicts to declare.

Acknowledgements

References

1 L. Gherardini, G. Ciuti, S. Tognarelli and C. Cinti, Searching for the perfect wave: The effect of radiofrequency electromagnetic fields on cells, *Int. J. Mol. Sci.*, 2014, **15**(4), 5366–5387.

2 S. J. Beebe, Considering effects of nanosecond pulsed electric fields on proteins, *Bioelectrochemistry*, 2015, **103**, 52–59.

3 I. Bekard and D. E. Dunstan, Electric field induced changes in protein conformation, *Soft Matter*, 2014, **10**(3), 431–437.

4 L. Astrakas, C. Gousias and M. Tzaphlidou, Electric field effects on chignolin conformation, *J. Appl. Phys.*, 2011, **109**(9), 094702.

5 D. I. de Pomerai, B. Smith, A. Dawe, K. North, T. Smith, D. B. Archer, I. R. Duce, D. Jones and E. P. M. Candido, Microwave radiation can alter protein conformation without bulk heating, *FEBS Lett.*, 2003, **543**(1–3), 93–97.

6 J. A. Laurence, P. W. French, R. A. Lindner and D. R. McKenzie, Biological effects of electromagnetic fields-mechanisms for the effects of pulsed microwave radiation on protein conformation, *J. Theor. Biol.*, 2000, **206**(2), 291–298.

7 F. Lugli, F. Toschi, F. Biscarini and F. Zerbetto, Electric field effects on short fibrils of Aβ amyloid peptides, *J. Chem. Theory Comput.*, 2010, **6**(11), 3516–3526.

8 F. Mancinelli, M. Caraglia, A. Abbruzzese, G. d'Ambrosio, R. Massa and E. Bismuto, Non-thermal effects of electromagnetic fields at mobile phone frequency on the refolding of an intracellular protein: Myoglobin, *J. Cell. Biochem.*, 2004, **93**(1), 188–196.

9 T. Saliev, Z. Mustapova, G. Kulsharova, D. Bulanin and S. Mikhalovsky, Therapeutic potential of electromagnetic fields for tissue engineering and wound healing, *Cell Proliferation*, 2014, **47**(6), 485–493.

10 G. L.-Y. Cheing, X. Li, L. Huang, R. L.-C. Kwan and K.-K. Cheung, Pulsed electromagnetic fields (PEMF) promote early wound healing and myofibroblast proliferation in diabetic rats, *Bioelectromagnetics*, 2014, **35**(3), 161–169.

11 A. A. Pilla, Nonthermal electromagnetic fields: From first messenger to therapeutic applications, *Electromagn. Biol. Med.*, 2013, **32**(2), 123–136.

12 A. Cifuentes-Rius, A. Ivask, S. Das, N. Penya-Auladell, L. Fabregas, N. L. Fletcher, Z. H. Houston, K. J. Thurecht and N. H. Voelcker, Gold nanocluster-mediated cellular death under electromagnetic radiation, *ACS Appl. Mater. Interfaces*, 2017, **9**(47), 41159–41167.

13 L. Li, X. Guo, X. Peng, H. Zhang, Y. Liu, H. Li, X. He, D. Shi, B. Xiong, Y. Zhao, C. Zheng and X. Yang, Radiofrequency-responsive dual-valent gold nanoclusters for enhancing synergistic therapy of tumor ablation and artery embolization, *Nano Today*, 2020, **35**, 100934–100946.

14 S. P. Loughran, M. S. Al Hossain, A. Bentvelzen, M. Elwood, J. Finnie, J. Horvat, S. Iskra, E. P. Ivanova, J. Manavis, C. K. Mudiyanselage, A. Lajevardipour, B. Martinac, R. McIntosh, R. McKenzie, M. Mustapic, Y. Nakayama, E. Pirogova, M. H. Rashid, N. A. Taylor, N. Todorova, P. M. Wiedemann, R. Vink, A. Wood, I. Yarovsky and R. J. Croft, Bioelectromagnetics research within an Australian context: The Australian centre for electromagnetic bioeffects research (ACEBR), *Int. J. Environ. Res. Public Health*, 2016, **13**(10), 967–981.

15 G. W. Arendash, Review of the evidence that transcranial electromagnetic treatment will be a safe and effective therapeutic against Alzheimer's disease, *J. Alzheimer's Dis.*, 2016, **53**(3), 753–771.

16 L. Chopinet and M. P. Rols, Nanosecond electric pulses: a mini-review of the present state of the art, *Bioelectrochemistry*, 2015, **103**, 2–6.

17 N. J. English and C. J. Waldron, Perspectives on external electric fields in molecular simulation: progress, prospects and challenges, *Phys. Chem. Chem. Phys.*, 2015, **17**(19), 12407–12440.

18 S. Shaik, D. Danovich, J. Joy, Z. Wang and T. Stuyver, Electric-field mediated chemistry: uncovering and exploiting the potential of (oriented) electric fields to exert chemical catalysis and reaction control, *J. Am. Chem. Soc.*, 2020, **142**(29), 12551–12562.

19 S. Shaik, R. Ramanan, D. Danovich and D. Mandal, Structure and reactivity/selectivity control by oriented-external electric fields, *Chem. Soc. Rev.*, 2018, **47**(14), 5125–5145.

20 T. Stuyver, D. Danovich, J. Joy and S. Shaik, External electric field effects on chemical structure and reactivity, *Wiley Interdiscip. Rev.: Comput. Mol. Sci.*, 2020, **10**(2), e1438.

21 S. Ciampi, N. Darwish, H. M. Aitken, I. Díez-Pérez and M. L. Coote, Harnessing electrostatic catalysis in single molecule, electrochemical and chemical systems: A rapidly growing experimental tool box, *Chem. Soc. Rev.*, 2018, **47**(14), 5146–5164.

22 *Effects of Electric Fields on Structure and Reactivity: New Horizons in Chemistry,* ed. S. Shaik and T. Stuyver, Royal Society of Chemistry, Cambridge, UK, 2021.

23 M. Alemani, M. V. Peters, S. Hecht, K.-H. Rieder, F. Moresco and L. Grill, Electric field-induced isomerization of azobenzene by STM, *J. Am. Chem. Soc.*, 2006, **128**(45), 14446–14447.

This journal is © the Owner Societies 2022

Phys. Chem. Chem. Phys., 2022, **24**, 6327–6348 | **6341**

24 D. H. Murgida and P. Hildebrandt, Electron-transfer processes of cytochrome *c* at interfaces. New insights by surface-enhanced resonance Raman spectroscopy, *Acc. Chem. Res.*, 2004, **37**(11), 854–861.

25 S. D. Fried and S. G. Boxer, Electric fields and enzyme catalysis, *Annu. Rev. Biochem.*, 2017, **86**(1), 387–415.

26 C. F. Gorin, E. S. Beh, Q. M. Bui, G. R. Dick and M. W. Kanan, Interfacial electric field effects on a carbene reaction catalyzed by Rh porphyrins, *J. Am. Chem. Soc.*, 2013, **135**(30), 11257–11265.

27 N. Darwish, A. C. Aragonès, T. Darwish, S. Ciampi and I. Díez-Pérez, Multi-responsive photo- and chemo-electrical single-molecule switches, *Nano Lett.*, 2014, **14**(12), 7064–7070.

28 C. Geng, J. Li, T. Weiske, M. Schlangen, S. Shaik and H. Schwarz, Electrostatic and charge-induced methane activation by a concerted double C–H bond insertion, *J. Am. Chem. Soc.*, 2017, **139**(4), 1684–1689.

29 L. Yue, J. Li, S. Zhou, X. Sun, M. Schlangen, S. Shaik and H. Schwarz, Control of product distribution and mechanism by ligation and electric field in the thermal activation of methane, *Angew. Chem., Int. Ed.*, 2017, **56**(34), 10219–10223.

30 A. C. Aragonès, N. L. Haworth, N. Darwish, S. Ciampi, N. J. Bloomfield, G. G. Wallace, I. Diez-Perez and M. L. Coote, Electrostatic catalysis of a Diels–Alder reaction, *Nature*, 2016, **531**(7592), 88–91.

31 A. Warshel, Electrostatic basis of structure–function correlation in proteins, *Acc. Chem. Res.*, 1981, **14**(9), 284–290.

32 A. R. Finkelmann, M. T. Stiebritz and M. Reiher, Electric-field effects on the [FeFe]-hydrogenase active site, *Chem. Commun.*, 2013, **49**(73), 8099–8101.

33 Extremely low frequency electric and magnetic fields, https://www.arpansa.gov.au/understanding-radiation/what-is-radiation/non-ionising-radiation/low-frequency-electric-magnetic-fields (accessed 27th October).

34 N. J. English and J. M. D. MacElroy, Hydrogen bonding and molecular mobility in liquid water in external electromagnetic fields, *J. Chem. Phys.*, 2003, **119**(22), 11806–11813.

35 W. Tourab and A. Babouri, Measurement and modeling of personal exposure to the electric and magnetic fields in the vicinity of high voltage power lines, *Saf. Health Work*, 2016, **7**(2), 102–110.

36 R. J. Clarke, The dipole potential of phospholipid membranes and methods for its detection, *Adv. Colloid Interface Sci.*, 2001, **89–90**, 263–281.

37 L. Wang, Measurements and implications of the membrane dipole potential, *Annu. Rev. Biochem.*, 2012, **81**(1), 615–635.

38 R. Nuccitelli, X. Chen, A. G. Pakhomov, W. H. Baldwin, S. Sheikh, J. L. Pomicter, W. Ren, C. Osgood, R. J. Swanson, J. F. Kolb, S. J. Beebe and K. H. Schoenbach, A new pulsed electric field therapy for melanoma disrupts the tumor's blood supply and causes complete remission without recurrence, *Int. J. Cancer*, 2009, **125**(2), 438–445.

39 B. Al-Sakere, F. André, C. Bernat, E. Connault, P. Opolon, R. V. Davalos, B. Rubinsky and L. M. Mir, Tumor ablation with irreversible electroporation, *PLoS One*, 2007, **2**(11), e1135.

40 J. Zhang, P. F. Blackmore, B. Y. Hargrave, S. Xiao, S. J. Beebe and K. H. Schoenbach, Nanosecond pulse electric field (nanopulse): A novel non-ligand agonist for platelet activation, *Arch. Biochem. Biophys.*, 2008, **471**(2), 240–248.

41 B. Ferraro, Y. L. Cruz, D. Coppola and R. Heller, Intradermal delivery of plasmid VEGF165 by electroporation promotes wound healing, *Mol. Ther.*, 2009, **17**(4), 651–657.

42 R. V. Davalos, L. M. Mir and B. Rubinsky, Tissue ablation with irreversible electroporation, *Ann. Biomed. Eng.*, 2005, **33**(2), 223.

43 J. A. Stroscio and D. M. Eigler, Atomic and molecular manipulation with the scanning tunneling microscope, *Science*, 1991, **254**(5036), 1319–1326.

44 Y. A. Hong, J. R. Hahn and H. Kang, Electron transfer through interfacial water layer studied by scanning tunneling microscopy, *J. Chem. Phys.*, 1998, **108**(11), 4367–4370.

45 S. Ilieva, D. Cheshmedzhieva and T. Dudev, Electric field influence on the helical structure of peptides: Insights from DFT/PCM computations, *Phys. Chem. Chem. Phys.*, 2019, **21**(29), 16198–16206.

46 R. M. Rodrigues, Z. Avelar, L. Machado, R. N. Pereira and A. A. Vicente, Electric field effects on proteins – Novel perspectives on food and potential health implications, *Food Res. Int.*, 2020, **137**, 109709.

47 G. Pandey, S. Morla, H. B. Nemade, S. Kumar and V. Ramakrishnan, Modulation of aggregation with an electric field; scientific roadmap for a potential non-invasive therapy against tauopathies, *RSC Adv.*, 2019, **9**(9), 4744–4750.

48 Y. Lu, X. F. Shi, F. R. Salsbury, Jr. and P. Derreumaux, Influence of electric field on the amyloid-beta(29-42) peptides embedded in a membrane bilayer, *J. Chem. Phys.*, 2018, **148**(4), 045105.

49 Y. Xie, Y. Pan, R. Zhang, Y. Liang and Z. Li, Modulating protein behaviors on responsive surface by external electric fields: A molecular dynamics study, *Appl. Surf. Sci.*, 2015, **326**, 55–65.

50 X. Wang, Y. Li, X. He, S. Chen and J. Z. H. Zhang, Effect of strong electric field on the conformational integrity of insulin, *J. Phys. Chem. A*, 2014, **118**(39), 8942–8952.

51 L. G. Astrakas, C. Gousias and M. Tzaphlidou, Structural destabilization of chignolin under the influence of oscillating electric fields, *J. Appl. Phys.*, 2012, **111**(7), 074702.

52 N. J. English and D. A. Mooney, Denaturation of hen egg white lysozyme in electromagnetic fields: a molecular dynamics study, *J. Chem. Phys.*, 2007, **126**(9), 091105.

53 A. Budi, F. S. Legge, H. Treutlein and I. Yarovsky, Electric field effects on insulin chain-B conformation, *J. Phys. Chem. B*, 2005, **109**(47), 22641–22648.

54 M. Porcelli, G. Cacciapuoti, S. Fusco, R. Massa, G. d'Ambrosio, C. Bertoldo, M. De Rosa and V. Zappia, Non-thermal effects of microwaves on proteins: thermophilic enzymes as model system, *FEBS Lett.*, 1997, **402**(2–3), 102–106.

6342 | *Phys. Chem. Chem. Phys.*, 2022, **24**, 6327–6348

This journal is © the Owner Societies 2022

55 R. L. Redler, D. Shirvanyants, O. Dagliyan, F. Ding, D. N. Kim, P. Kota, E. A. Proctor, S. Ramachandran, A. Tandon and N. V. Dokholyan, Computational approaches to understanding protein aggregation in neurodegeneration, *J. Mol. Cell Biol.*, 2014, **6**(2), 104–115.

56 F. Chiti and C. M. Dobson, Protein misfolding, amyloid formation, and human disease: A summary of progress over the last decade, *Annu. Rev. Biochem.*, 2017, **86**, 27–68.

57 G. W. Arendash, C. Cao and J. Tan, Prevention and treatment of brain diseases and disorders related to abnormal protein aggregation through electromagnetic field treatment, US Pat., 9,238,149 B2. 2016.

58 A. Sinelnikova, T. Mandl, C. Ostlin, O. Granas, M. N. Brodmerkel, E. G. Marklund and C. Caleman, Reproducibility in the unfolding process of protein induced by an external electric field, *Chem. Sci.*, 2020, **12**(6), 2030–2038.

59 P. G. Tharushi Perera, N. Todorova, Z. Vilagosh, O. Bazaka, T. H. P. Nguyen, K. Bazaka, R. J. Crawford, R. J. Croft, I. Yarovsky and E. P. Ivanova, Translocation of silica nanospheres through giant unilamellar vesicles (GUVs) induced by a high frequency electromagnetic field, *RSC Adv.*, 2021, **11**(50), 31408–31420.

60 J. P. Cerón-Carrasco and D. Jacquemin, Electric-field induced mutation of DNA: a theoretical investigation of the GC base pair, *Phys. Chem. Chem. Phys.*, 2013, **15**(13), 4548–4553.

61 J. P. Cerón-Carrasco and D. Jacquemin, Electric field induced DNA damage: an open door for selective mutations, *Chem. Commun.*, 2013, **49**(69), 7578–7580.

62 J. P. Cerón-Carrasco, J. Cerezo and D. Jacquemin, How DNA is damaged by external electric fields: Selective mutation vs. random degradation, *Phys. Chem. Chem. Phys.*, 2014, **16**(18), 8243–8246.

63 D. Rai, A. D. Kulkarni, S. P. Gejji, L. J. Bartolotti and R. K. Pathak, Exploring electric field induced structural evolution of water clusters, $(H_2O)n$ [n = 9–20]: Density functional approach, *J. Chem. Phys.*, 2013, **138**(4), 044304.

64 N. Todorova, A. Bentvelzen, N. J. English and I. Yarovsky, Electromagnetic-field effects on structure and dynamics of amyloidogenic peptides, *J. Chem. Phys.*, 2016, **144**(8), 085101.

65 J. Baker, Molecular structure and vibrational spectra, in *Handbook of Computational Chemistry*, ed. J. Leszczynski, A. Kaczmarek-Kedziera, T. Puzyn, G. M. Papadopoulos, H. Reis and K. M. Shukla, Springer International Publishing, Cham, 2017, pp. 423–496.

66 M. Jaszuński, A. Rizzo and K. Ruud, Molecular electric, magnetic, and optical properties, in *Handbook of Computational Chemistry*, ed. J. Leszczynski, A. Kaczmarek-Kedziera, T. Puzyn, G. M. Papadopoulos, H. Reis and K. M.Shukla, Springer International Publishing, Cham, 2017, pp. 497–592.

67 M. Springborg, M. Molayem and B. Kirtman, The response of extended systems to electrostatic fields, in *Handbook of Computational Chemistry*, ed. J. Leszczynski, A. Kaczmarek-Kedziera, T. Puzyn, G. M. Papadopoulos, H. Reis and K. M. Shukla, Springer International Publishing, Cham, 2017, pp. 1415–1458.

68 P. G. Mezey, *Potential Energy Hypersurfaces*, Elsevier, Amsterdam, 1987.

69 D. J. Wales, *Energy Landscapes*, Cambridge University Press, Cambridge, UK, 2003.

70 R. Dovesi, B. Kirtman, L. Maschio, J. Maul, F. Pascale and M. Rérat, Calculation of the infrared intensity of crystalline systems. A comparison of three strategies based on berry phase, wannier function, and coupled-perturbed Kohn–Sham methods, *J. Phys. Chem. C*, 2019, **123**(13), 8336–8346.

71 J. Neugebauer, M. Reiher, C. Kind and B. A. Hess, Quantum chemical calculation of vibrational spectra of large molecules—Raman and IR spectra for Buckminsterfullerene, *J. Comput. Chem.*, 2002, **23**(9), 895–910.

72 J. Zheng, T. Yu, E. Papajak, I. M. Alecu, S. L. Mielke and D. G. Truhlar, Practical methods for including torsional anharmonicity in thermochemical calculations on complex molecules: The internal-coordinate multi-structural approximation, *Phys. Chem. Chem. Phys.*, 2011, **13**(23), 10885–10907.

73 P. T. Panek and C. R. Jacob, Anharmonic theoretical vibrational spectroscopy of polypeptides, *J. Phys. Chem. Lett.*, 2016, **7**(16), 3084–3090.

74 Y. Cornaton, M. Ringholm, O. Louant and K. Ruud, Analytic calculations of anharmonic infrared and Raman vibrational spectra, *Phys. Chem. Chem. Phys.*, 2016, **18**(5), 4201–4215.

75 M. J. Frisch, G. W. Trucks, H. B. Schlegel, G. E. Scuseria, M. A. Robb, J. R. Cheeseman, G. Scalmani, V. Barone, G. A. Petersson, H. Nakatsuji, X. Li, M. Caricato, A. V. Marenich, J. Bloino, B. G. Janesko, R. Gomperts, B. Mennucci, H. P. Hratchian, J. V. Ortiz, A. F. Izmaylov, J. L. Sonnenberg, D. Williams-Young, F. Ding, F. Lipparini, F. Egidi, J. Goings, B. Peng, A. Petrone, T. Henderson, D. Ranasinghe, V. G. Zakrzewski, J. Gao, N. Rega, G. Zheng, W. Liang, M. Hada, M. Ehara, K. Toyota, R. Fukuda, J. Hasegawa, M. Ishida, T. Nakajima, Y. Honda, O. Kitao, H. Nakai, T. Vreven, K. Throssell, J. A. Montgomery Jr., J. E. Peralta, F. Ogliaro, M. J. Bearpark, J. J. Heyd, E. N. Brothers, K. N. Kudin, V. N. Staroverov, T. A. Keith, R. Kobayashi, J. Normand, K. Raghavachari, A. P. Rendell, J. C. Burant, S. S. Iyengar, J. Tomasi, M. Cossi, J. M. Millam, M. Klene, C. Adamo, R. Cammi, J. W. Ochterski, R. L. Martin, K. Morokuma, O. Farkas, J. B. Foresman and D. J. Fox, *Gaussian 16 Rev. C.01*, Wallingford, CT, 2016.

76 Y. Shao, Z. Gan, E. Epifanovsky, A. T. B. Gilbert, M. Wormit, J. Kussmann, A. W. Lange, A. Behn, J. Deng, X. Feng, D. Ghosh, M. Goldey, P. R. Horn, L. D. Jacobson, I. Kaliman, R. Z. Khaliullin, T. Kuś, A. Landau, J. Liu, E. I. Proynov, Y. M. Rhee, R. M. Richard, M. A. Rohrdanz, R. P. Steele, E. J. Sundstrom, H. L. Woodcock, P. M. Zimmerman, D. Zuev, B. Albrecht, E. Alguire, B. Austin, G. J. O. Beran, Y. A. Bernard, E. Berquist, K. Brandhorst, K. B. Bravaya, S. T. Brown, D. Casanova, C.-M. Chang, Y. Chen, S. H. Chien, K. D. Closser, D. L. Crittenden, M. Diedenhofen, R. A. DiStasio, H. Do, A. D. Dutoi, R. G. Edgar, S. Fatehi, L. Fusti-Molnar, A. Ghysels, A. Golubeva-Zadorozhnaya, J. Gomes,

This journal is © the Owner Societies 2022

Phys. Chem. Chem. Phys., 2022, **24**, 6327–6348 | **6343**

M. W. D. Hanson-Heine, P. H. P. Harbach, A. W. Hauser, E. G. Hohenstein, Z. C. Holden, T.-C. Jagau, H. Ji, B. Kaduk, K. Khistyaev, J. Kim, J. Kim, R. A. King, P. Klunzinger, D. Kosenkov, T. Kowalczyk, C. M. Krauter, K. U. Lao, A. D. Laurent, K. V. Lawler, S. V. Levchenko, C. Y. Lin, F. Liu, E. Livshits, R. C. Lochan, A. Luenser, P. Manohar, S. F. Manzer, S.-P. Mao, N. Mardirossian, A. V. Marenich, S. A. Maurer, N. J. Mayhall, E. Neuscamman, C. M. Oana, R. Olivares-Amaya, D. P. O'Neill, J. A. Parkhill, T. M. Perrine, R. Peverati, A. Prociuk, D. R. Rehn, E. Rosta, N. J. Russ, S. M. Sharada, S. Sharma, D. W. Small, A. Sodt, T. Stein, D. Stück, Y.-C. Su, A. J. W. Thom, T. Tsuchimochi, V. Vanovschi, L. Vogt, O. Vydrov, T. Wang, M. A. Watson, J. Wenzel, A. White, C. F. Williams, J. Yang, S. Yeganeh, S. R. Yost, Z.-Q. You, I. Y. Zhang, X. Zhang, Y. Zhao, B. R. Brooks, G. K. L. Chan, D. M. Chipman, C. J. Cramer, W. A. Goddard, M. S. Gordon, W. J. Hehre, A. Klamt, H. F. Schaefer, M. W. Schmidt, C. D. Sherrill, D. G. Truhlar, A. Warshel, X. Xu, A. Aspuru-Guzik, R. Baer, A. T. Bell, N. A. Besley, J.-D. Chai, A. Dreuw, B. D. Dunietz, T. R. Furlani, S. R. Gwaltney, C.-P. Hsu, Y. Jung, J. Kong, D. S. Lambrecht, W. Liang, C. Ochsenfeld, V. A. Rassolov, L. V. Slipchenko, J. E. Subotnik, T. Van Voorhis, J. M. Herbert, A. I. Krylov, P. M. W. Gill and M. Head-Gordon, Advances in molecular quantum chemistry contained in the Q-Chem 4 program package, *Mol. Phys.*, 2015, **113**(2), 184–215.

77 S. G. Balasubramani, G. P. Chen, S. Coriani, M. Diedenhofen, M. S. Frank, Y. J. Franzke, F. Furche, R. Grotjahn, M. E. Harding, C. Hättig, A. Hellweg, B. Helmich-Paris, C. Holzer, U. Huniar, M. Kaupp, A. M. Khah, S. K. Khani, T. Müller, F. Mack, B. D. Nguyen, S. M. Parker, E. Perlt, D. Rappoport, K. Reiter, S. Roy, M. Rückert, G. Schmitz, M. Sierka, E. Tapavicza, D. P. Tew, C. v. Wüllen, V. K. Voora, F. Weigend, A. Wodyński and J. M. Yu, TURBOMOLE: Modular program suite for ab initio quantum-chemical and condensed-matter simulations, *J. Chem. Phys.*, 2020, **152**(18), 184107.

78 T. Stuyver, J. Huang, D. Mallick, D. Danovich and S. Shaik, TITAN: A code for modeling and generating electric fields—features and applications to enzymatic reactivity, *J. Comput. Chem.*, 2020, **41**(1), 74–82.

79 P. Umari and A. Pasquarello, Ab initio molecular dynamics in a finite homogeneous electric field, *Phys. Rev. Lett.*, 2002, **89**(15), 157602.

80 N. J. English and J. M. D. MacElroy, Molecular dynamics simulations of microwave heating of water, *J. Chem. Phys.*, 2003, **118**(4), 1589–1592.

81 M. J. Abraham, T. Murtola, R. Schulz, S. Páll, J. C. Smith, B. Hess and E. Lindahl, GROMACS: High performance molecular simulations through multi-level parallelism from laptops to supercomputers, *SoftwareX*, 2015, **1-2**, 19–25.

82 J. C. Phillips, D. J. Hardy, J. D. C. Maia, J. E. Stone, J. V. Ribeiro, R. C. Bernardi, R. Buch, G. Fiorin, J. Henin, W. Jiang, R. McGreevy, M. C. R. Melo, B. K. Radak, R. D. Skeel, A. Singharoy, Y. Wang, B. Roux, A. Aksimentiev, Z. Luthey-Schulten, L. V. Kale, K. Schulten, C. Chipot and E. Tajkhorshid, Scalable molecular dynamics on CPU and GPU architectures with NAMD, *J. Chem. Phys.*, 2020, **153**(4), 044130.

83 S. Plimpton, Fast parallel algorithms for short-range molecular dynamics, *J. Comput. Phys.*, 1995, **117**(1), 1–19.

84 I. T. Todorov, W. Smith, K. Trachenko and M. T. Dove, DL_POLY_3: New dimensions in molecular dynamics simulations via massive parallelism, *J. Mater. Chem.*, 2006, **16**, 20.

85 K. Khajeh, H. Aminfar, Y. Masuda and M. Mohammadpourfard, Implementation of magnetic field force in molecular dynamics algorithm: NAMD source code version 2.12, *J. Mol. Model.*, 2020, **26**(5), 106.

86 X. Chen, L. Hou, W. Li, S. Li and Y. Chen, Molecular dynamics simulation of magnetic field influence on waxy crude oil, *J. Mol. Liq.*, 2018, **249**, 1052–1059.

87 N. J. English, G. Y. Solomentsev and P. O'Brien, Nonequilibrium molecular dynamics study of electric and low-frequency microwave fields on hen egg white lysozyme, *J. Chem. Phys.*, 2009, **131**(3), 035106.

88 S. Acosta-Gutierrez, J. Hernandez-Rojas, J. Breton, J. M. Llorente and D. J. Wales, Physical properties of small water clusters in low and moderate electric fields, *J. Chem. Phys.*, 2011, **135**(12), 124303.

89 F. H. Song, B. Q. Li and C. Liu, Molecular dynamics simulation of nanosized water droplet spreading in an electric field, *Langmuir*, 2013, **29**(13), 4266–4274.

90 R. Ludwig, Water: From clusters to the bulk, *Angew. Chem., Int. Ed.*, 2001, **40**(10), 1808–1827.

91 R. Reale, N. J. English, P. Marracino, M. Liberti and F. Apollonio, Dipolar response and hydrogen-bond kinetics in liquid water in square-wave time-varying electric fields, *Mol. Phys.*, 2013, **112**(14), 1870–1878.

92 Z. Futera and N. J. English, Electric-field effects on adsorbed-water structural and dynamical properties at rutile- and anatase-TiO2 surfaces, *J. Phys. Chem. C*, 2016, **120**(35), 19603–19612.

93 Y. C. Choi, C. Pak and K. S. Kim, Electric field effects on water clusters (*n* = 3–5): Systematic ab initio study of structures, energetics, and transition states, *J. Chem. Phys.*, 2006, **124**(9), 094308.

94 D. Rai, A. D. Kulkarni, S. P. Gejji and R. K. Pathak, Water clusters (H2O)n, n = 6–8, in external electric fields, *J. Chem. Phys.*, 2008, **128**(3), 034310.

95 E. J. L. Toledo, R. Custodio, T. C. Ramalho, M. E. G. Porto and Z. M. Magriotis, Electrical field effects on dipole moment, structure and energetic of (H2O)n (2 ≤ n ≤ 15) cluster, *THEOCHEM*, 2009, **915**(1), 170–177.

96 M. Karahka and H. J. Kreuzer, Water whiskers in high electric fields, *Phys. Chem. Chem. Phys.*, 2011, **13**(23), 11027–11033.

97 L. J. Bartolotti, D. Rai, A. D. Kulkarni, S. P. Gejji and R. K. Pathak, Water clusters (H2O)n [n = 9–20] in external

6344 | *Phys. Chem. Chem. Phys.*, 2022, **24**, 6327–6348

This journal is © the Owner Societies 2022

electric fields: Exotic OH stretching frequencies near breakdown, *Comput. Theor. Chem.*, 2014, **1044**, 66–73.

98 Y. Bai, H.-M. He, Y. Li, Z.-R. Li, Z.-J. Zhou, J.-J. Wang, D. Wu, W. Chen, F.-L. Gu, B. G. Sumpter and J. Huang, Electric field effects on the intermolecular interactions in water whiskers: Insight from structures, energetics, and properties, *J. Phys. Chem. A*, 2015, **119**(10), 2083–2090.

99 W. Zhao, H. Huang, Q. Bi, Y. Xu and Y. Lü, One-dimensional water nanowires induced by electric fields, *Phys. Chem. Chem. Phys.*, 2019, **21**(35), 19414–19422.

100 N. D. Gurav, S. P. Gejji, L. J. Bartolotti and R. K. Pathak, Encaged molecules in external electric fields: A molecular "tug-of-war", *J. Chem. Phys.*, 2016, **145**(7), 074302.

101 C. D. Daub, P.-O. Åstrand and F. Bresme, Lithium ion–water clusters in strong electric fields: A quantum chemical study, *J. Phys. Chem. A*, 2015, **119**(20), 4983–4992.

102 G. Cassone, F. Creazzo, P. V. Giaquinta, J. Sponer and F. Saija, Ionic diffusion and proton transfer in aqueous solutions of alkali metal salts, *Phys. Chem. Chem. Phys.*, 2017, **19**(31), 20420–20429.

103 G. Cassone, F. Creazzo and F. Saija, Ionic diffusion and proton transfer of $MgCl_2$ and $CaCl_2$ aqueous solutions: an ab initio study under electric field, *Mol. Simul.*, 2019, **45**(4–5), 373–380.

104 Z. Futera and N. J. English, Communication: Influence of external static and alternating electric fields on water from long-time non-equilibrium ab initio molecular dynamics, *J. Chem. Phys.*, 2017, **147**(3), 031102.

105 J. H. Lee, C. Kim, M. Tokman and M. E. Colvin, Energy component analysis of electric field-induced shape change in water nanodroplets, *J. Phys. Chem. C*, 2021, **125**(12), 6933–6944.

106 R. Reale, N. J. English, P. Marracino, M. Liberti and F. Apollonio, Translational and rotational diffusive motion in liquid water in square-wave time-varying electric fields, *Chem. Phys. Lett.*, 2013, **582**, 60–65.

107 M. Avena, P. Marracino, M. Liberti, F. Apollonio and N. J. English, Communication: influence of nanosecond-pulsed electric fields on water and its subsequent relaxation: dipolar effects and debunking memory, *J. Chem. Phys.*, 2015, **142**(14), 141101.

108 M. F. Chaplin, The memory of water: An overview, *Homeopathy*, 2007, **96**(3), 143–150.

109 S. J. Boyd, Y. Krishnan, M. R. Ghaani and N. J. English, Influence of external static and alternating electric fields on self-diffusion of water from molecular dynamics, *J. Mol. Liq.*, 2021, 327.

110 Y. Liu, K. Huang, Y. Zhou, D. Gou and H. Shi, Hydrogen bonding and the structural properties of glycerol-water mixtures with a microwave field: A molecular dynamics study, *J. Phys. Chem. B*, 2021, **125**(29), 8099–8106.

111 N. Li, Z. Sun, Y. Fan, W. Liu, Y. Guo, B. Li and Z. Wang, Understanding the breakup mechanism of a droplet under a DC electric field with molecular dynamics simulations and weak interaction analysis, *J. Mol. Liq.*, 2021, 321.

112 F. Song, H. Niu, J. Fan, Q. Chen, G. Wang and L. Liu, Molecular dynamics study on the coalescence and break-up behaviors of ionic droplets under DC electric field, *J. Mol. Liq.*, 2020, 312.

113 R. Shi and Y. Wang, Surface structure of ionic liquids under an external electric field, *Mol. Simul.*, 2017, **43**(13–16), 1295–1299.

114 M. T. Nguyen and Q. Shao, Effect of zwitterionic molecules on ionic transport under electric fields: A molecular simulation study, *J. Chem. Eng. Data*, 2019, **65**(2), 385–395.

115 D. Bedrov, J. P. Piquemal, O. Borodin, A. D. MacKerell, Jr., B. Roux and C. Schroder, Molecular dynamics simulations of ionic liquids and electrolytes using polarizable force fields, *Chem. Rev.*, 2019, **119**(13), 7940–7995.

116 P. Raiteri, P. Kraus and J. D. Gale, Molecular dynamics simulations of liquid-liquid interfaces in an electric field: The water-1,2-dichloroethane interface, *J. Chem. Phys.*, 2020, **153**(16), 164714.

117 J. Peng, D. Cao, Z. He, J. Guo, P. Hapala, R. Ma, B. Cheng, J. Chen, W. J. Xie, X.-Z. Li, P. Jelínek, L.-M. Xu, Y. Q. Gao, E.-G. Wang and Y. Jiang, The effect of hydration number on the interfacial transport of sodium ions, *Nature*, 2018, **557**(7707), 701–705.

118 Z. Wang, Y. Yang, D. L. Olmsted, M. Asta and B. B. Laird, Evaluation of the constant potential method in simulating electric double-layer capacitors, *J. Chem. Phys.*, 2014, **141**(18), 184102.

119 S. Bonakala and M. I. Hasan, Comparative study of external electric field and potential effects on liquid water ions, *Mol. Phys.*, 2021, e1998689.

120 P.-O. Löwdin, Proton tunneling in DNA and its biological implications, *Rev. Mod. Phys.*, 1963, **35**(3), 724–732.

121 P. O. Löwdin, *Electronic aspects of biochemistry*, Academic Press, New York, 1964.

122 D. Jacquemin, J. Zúñiga, A. Requena and J. P. Céron-Carrasco, Assessing the importance of proton transfer reactions in DNA, *Acc. Chem. Res.*, 2014, **47**(8), 2467–2474.

123 J. Xue, X. Guo, X. Wang and Y. Xiao, Density functional theory studies on cytosine analogues for inducing double-proton transfer with guanine, *Sci. Rep.*, 2020, **10**(1), 9671.

124 A. Kumar and M. D. Sevilla, Proton-coupled electron transfer in DNA on formation of radiation-produced ion radicals, *Chem. Rev.*, 2010, **110**(12), 7002–7023.

125 J. P. Céron-Carrasco, D. Jacquemin and E. Cauët, Cisplatin cytotoxicity: A theoretical study of induced mutations, *Phys. Chem. Chem. Phys.*, 2012, **14**(36), 12457–12464.

126 A. Galano and J. R. Alvarez-Idaboy, On the evolution of one-electron-oxidized deoxyguanosine in damaged DNA under physiological conditions: a DFT and ONIOM study on proton transfer and equilibrium, *Phys. Chem. Chem. Phys.*, 2012, **14**(36), 12476–12484.

127 J. Florián and J. Leszczyński, Spontaneous DNA mutations induced by proton transfer in the guanine·cytosine base pairs: An energetic perspective, *J. Am. Chem. Soc.*, 1996, **118**(12), 3010–3017.

128 J. P. Céron-Carrasco, A. Requena, J. Zúñiga, C. Michaux, E. A. Perpète and D. Jacquemin, Intermolecular proton transfer in microhydrated guanine−cytosine base pairs: A

This journal is © the Owner Societies 2022

Phys. Chem. Chem. Phys., 2022, **24**, 6327–6348 | **6345**

new mechanism for spontaneous mutation in DNA, *J. Phys. Chem. A*, 2009, **113**(39), 10549–10556.

129 K. H. Schoenbach, R. P. Joshi, J. F. Kolb, C. Nianyong, M. Stacey, P. F. Blackmore, E. S. Buescher and S. J. Beebe, Ultrashort electrical pulses open a new gateway into biological cells, *Proc. IEEE*, 2004, **92**(7), 1122–1137.

130 T. Batista Napotnik, M. Reberšek, P. T. Vernier, B. Mali and D. Miklavčič, Effects of high voltage nanosecond electric pulses on eukaryotic cells (*in vitro*): A systematic review, *Bioelectrochemistry*, 2016, **110**, 1–12.

131 D. Miklavčič, G. Serša, E. Brecelj, J. Gehl, D. Soden, G. Bianchi, P. Ruggieri, C. R. Rossi, L. G. Campana and T. Jarm, Electrochemotherapy: Technological advancements for efficient electroporation-based treatment of internal tumors, *Med. Biol. Eng. Comput.*, 2012, **50**(12), 1213–1225.

132 S. J. Beebe, Bioelectrics in basic science and medicine: Impact of electric fields on cellular structures and functions, *J. Nanomed. Nanotechnol.*, 2013, **4**(2), 1000163–1000171.

133 M. Zhang, Z. Xiong, W. Chen, C. Yao, Z. Zhao and Y. Hua, Intense picosecond pulsed electric fields inhibit proliferation and induce apoptosis of HeLa cells, *Mol. Med. Rep.*, 2013, **7**, 1938–1944.

134 A. A. Arabi and C. F. Matta, Effects of external electric fields on double proton transfer kinetics in the formic acid dimer, *Phys. Chem. Chem. Phys.*, 2011, **13**(30), 13738–13748.

135 J. P. Cerón-Carrasco and D. Jacquemin, Influence of Mg^{2+} on the guanine–cytosine tautomeric equilibrium: Simulations of the induced intermolecular proton transfer, *Chem. Phys. Chem.*, 2011, **12**(14), 2615–2623.

136 A. A. Arabi and C. F. Matta, Adenine–thymine tautomerization under the influence of strong homogeneous electric fields, *Phys. Chem. Chem. Phys.*, 2018, **20**(18), 12406–12412.

137 A. A. Arabi and C. F. Matta, Effects of intense electric fields on the double proton transfer in the Watson–Crick Guanine–Cytosine base pair, *J. Phys. Chem. B*, 2018, **122**(37), 8631–8641.

138 A. Gheorghiu, P. V. Coveney and A. A. Arabi, The influence of external electric fields on proton transfer tautomerism in the guanine–cytosine base pair, *Phys. Chem. Chem. Phys.*, 2021, **23**(10), 6252–6265.

139 D. Rhodes and H. J. Lipps, G-quadruplexes and their regulatory roles in biology, *Nucleic Acids Res.*, 2015, **43**(18), 8627–8637.

140 J. P. Cerón-Carrasco and D. Jacquemin, Exposing the G-quadruplex to electric fields: The role played by telomeres in the propagation of DNA errors, *Phys. Chem. Chem. Phys.*, 2017, **19**(14), 9358–9365.

141 B. Mir, I. Serrano, D. Buitrago, M. Orozco, N. Escaja and C. González, Prevalent sequences in the human genome can form mini i-Motif structures at physiological pH, *J. Am. Chem. Soc.*, 2017, **139**(40), 13985–13988.

142 M. Zeraati, D. B. Langley, P. Schofield, A. L. Moye, R. Rouet, W. E. Hughes, T. M. Bryan, M. E. Dinger and D. Christ, I-motif DNA structures are formed in the nuclei of human cells, *Nat. Chem.*, 2018, **10**(6), 631–637.

143 J. P. Cerón-Carrasco and D. Jacquemin, i-Motif DNA structures upon electric field exposure: Completing the map of induced genetic errors, *Theor. Chem. Acc.*, 2019, **138**(3), 35.

144 N. Todorova and I. Yarovsky, The Enigma of amyloid forming proteins: Insights from molecular simulations*, *Aust. J. Chem.*, 2019, **72**(8), 574–584.

145 S. K. Vanga, J. Wang, A. Singh and V. Raghavan, Simulations of temperature and pressure unfolding in soy allergen Gly m 4 using molecular modeling, *J. Agric. Food Chem.*, 2019, **67**(45), 12547–12557.

146 M. Gladovic, C. Oostenbrink and U. Bren, Could microwave irradiation cause misfolding of peptides?, *J. Chem. Theory Comput.*, 2020, **16**(4), 2795–2802.

147 A. Budi, S. Legge, H. Treutlein and I. Yarovsky, Effect of external stresses on protein conformation: A computer modelling study, *Eur. Biophys. J.*, 2004, **33**(2), 121–129.

148 F. S. Legge, A. Budi, H. Treutlein and I. Yarovsky, Protein flexibility: Multiple molecular dynamics simulations of insulin chain B, *Biophys. Chem.*, 2006, **119**(2), 146–157.

149 K. J. Jalkanen, R. M. Nieminen, K. Frimand, J. Bohr, H. Bohr, R. C. Wade, E. Tajkhorshid and S. Suhai, A comparison of aqueous solvent models used in the calculation of the Raman and ROA spectra of l-alanine, *Chem. Phys.*, 2001, **265**(2), 125–151.

150 K. J. Jalkanen, M. Elstner and S. Suhai, Amino acids and small peptides as building blocks for proteins: Comparative theoretical and spectroscopic studies, *THEOCHEM*, 2004, **675**(1), 61–77.

151 J. Kubelka, R. A. G. D. Silva and T. A. Keiderling, Discrimination between peptide 310- and α-helices. Theoretical analysis of the impact of α-methyl substitution on experimental spectra, *J. Am. Chem. Soc.*, 2002, **124**(19), 5325–5332.

152 P. Bouř and T. A. Keiderling, Vibrational spectral simulation for peptides of mixed secondary structure: Method comparisons with the trpzip model hairpin, *J. Phys. Chem. B*, 2005, **109**(49), 23687–23697.

153 W. Chin, F. Piuzzi, J. P. Dognon, I. Dimicoli and M. Mons, Gas-phase models of γ turns: Effect of side-chain/backbone interactions investigated by IR/UV spectroscopy and quantum chemistry, *J. Chem. Phys.*, 2005, **123**(8), 84301.

154 R. Wałesa, T. Kupka and M. A. Broda, Density functional theory (DFT) prediction of structural and spectroscopic parameters of cytosine using harmonic and anharmonic approximations, *Struct. Chem.*, 2015, **26**(4), 1083–1093.

155 A. E. Williams, N. I. Hammer, R. C. Fortenberry and D. N. Reinemann, Tracking the amide i and αcoo− terminal ν(C = O) Raman bands in a family of l-glutamic acid-containing peptide fragments: A Raman and dft study, *Molecules*, 2021, **26**, 16.

156 K. J. Jalkanen, I. M. Degtyarenko, R. M. Nieminen, X. Cao, L. A. Nafie, F. Zhu and L. D. Barron, Role of hydration in determining the structure and vibrational spectra of L-alanine and N-acetyl L-alanine N′-methylamide in aqueous solution: A combined theoretical and experimental approach, *Theor. Chem. Acc.*, 2008, **119**(1–3), 191–210.

157 E. Deplazes, W. Van Bronswijk, F. Zhu, L. D. Barron, S. Ma, L. A. Nafie and K. J. Jalkanen, A combined theoretical and

6346 | *Phys. Chem. Chem. Phys.*, 2022, **24**, 6327–6348

This journal is © the Owner Societies 2022

experimental study of the structure and vibrational absorption, vibrational circular dichroism, Raman and Raman optical activity spectra of the L-histidine zwitterion, *Theor. Chem. Acc.*, 2008, **119**(1–3), 155–176.

158 T. A. Keiderling, Structure of condensed phase peptides: Insights from vibrational circular dichroism and Raman optical activity techniques, *Chem. Rev.*, 2020, **120**(7), 3381–3419.

159 B. J. Dutta, N. Sarmah and P. K. R. Bhattacharyya, On the effect of external perturbation on amino acid salt bridge: A DFT study, *J. Chem. Sci.*, 2017, **129**(5), 533–541.

160 Z.-J. Zhou, X.-P. Li, Z.-B. Liu, Z.-R. Li, X.-R. Huang and C.-C. Sun, Electric field-driven acid–base chemistry: Proton transfer from acid (HCl) to base (NH3/H2O), *J. Phys. Chem. A*, 2011, **115**(8), 1418–1422.

161 S. Shaik, S. P. de Visser and D. Kumar, External electric field will control the selectivity of enzymatic-like bond activations, *J. Am. Chem. Soc.*, 2004, **126**(37), 11746–11749.

162 W. Lai, H. Chen, K.-B. Cho and S. Shaik, External electric field can control the catalytic cycle of cytochrome P450cam: A QM/MM study, *J. Phys. Chem. Lett.*, 2010, **1**(14), 2082–2087.

163 Q. K. Timerghazin and M. R. Talipov, Unprecedented external electric field effects on S-nitrosothiols: Possible mechanism of biological regulation?, *J. Phys. Chem. Lett.*, 2013, **4**(6), 1034–1038.

164 T. Dudev, S. Ilieva and L. Doudeva, How an electric field can modulate the metal ion selectivity of protein binding sites: Insights from DFT/PCM calculations, *Phys. Chem. Chem. Phys.*, 2018, **20**(38), 24633–24640.

165 A. Sinelnikova, T. Mandl, H. Agelii, O. Granas, E. G. Marklund, C. Caleman and E. De Santis, Protein orientation in time-dependent electric fields: Orientation before destruction, *Biophys. J.*, 2021, **120**(17), 3709–3717.

166 A. Budi, F. S. Legge, H. Treutlein and I. Yarovsky, Comparative study of insulin chain-B in isolated and monomeric environments under external stress, *J. Phys. Chem. B*, 2008, **112**(26), 7916–7924.

167 A. Budi, F. S. Legge, H. Treutlein and I. Yarovsky, Effect of frequency on insulin response to electric field stress, *J. Phys. Chem. B*, 2007, **111**(20), 5748–5756.

168 C. P. Samaranayake and S. K. Sastry, Molecular dynamics evidence for nonthermal effects of electric fields on pectin methylesterase activity, *Phys. Chem. Chem. Phys.*, 2021, **23**(26), 14422–14432.

169 E. Della Valle, P. Marracino, O. Pakhomova, M. Liberti and F. Apollonio, Nanosecond pulsed electric signals can affect electrostatic environment of proteins below the threshold of conformational effects: The case study of SOD1 with a molecular simulation study, *PLoS One*, 2019, **14**(8), e0221685.

170 C. R. Arbeitman, P. Rojas, P. Ojeda-May and M. E. Garcia, The SARS-CoV-2 spike protein is vulnerable to moderate electric fields, *Nat. Commun.*, 2021, **12**(1), 5407.

171 F. Chiti and C. M. Dobson, Protein misfolding, functional amyloid, and human disease, *Annu. Rev. Biochem.*, 2006, **75**, 333–366.

172 D. Willbold, B. Strodel, G. F. Schroder, W. Hoyer and H. Heise, Amyloid-type protein aggregation and prion-like

properties of amyloids, *Chem. Rev.*, 2021, **121**(13), 8285–8307.

173 S. Muscat, F. Stojceski and A. Danani, Elucidating the effect of static electric field on amyloid beta 1–42 supramolecular assembly, *J. Mol. Graph Model.*, 2020, **96**, 107535.

174 N. Todorova, A. Bentvelzen and I. Yarovsky, Electromagnetic field modulates aggregation propensity of amyloid peptides, *J. Chem. Phys.*, 2020, **152**(3), 035104.

175 Y. Lu, X. F. Shi, F. R. Salsbury, Jr. and P. Derreumaux, Small static electric field strength promotes aggregation-prone structures in amyloid-beta(29–42), *J. Chem. Phys.*, 2017, **146**(14), 145101.

176 M. L. Yarmush, A. Golberg, G. Sersa, T. Kotnik and D. Miklavcic, Electroporation-based technologies for medicine: principles, applications, and challenges, *Annu. Rev. Biomed. Eng.*, 2014, **16**, 295–320.

177 T. Kotnik, L. Rems, M. Tarek and D. Miklavcic, Membrane electroporation and electropermeabilization: Mechanisms and models, *Annu. Rev. Biophys.*, 2019, **48**, 63–91.

178 L. Delemotte and M. Tarek, Molecular dynamics simulations of lipid membrane electroporation, *J. Membr. Biol.*, 2012, **245**(9), 531–543.

179 K. Shimizu, H. Nakamura and S. Watano, MD simulation study of direct permeation of a nanoparticle across the cell membrane under an external electric field, *Nanoscale*, 2016, **8**(23), 11897–11906.

180 Y. Ikeda, H. Nakamura, S. Ohsaki and S. Watano, Direct translocation of a negatively charged nanoparticle across a negatively charged model cell membrane, *Phys. Chem. Chem. Phys.*, 2021, **23**(17), 10591–10599.

181 R. C. Burke, S. M. Bardet, L. Carr, S. Romanenko, D. Arnaud-Cormos, P. Leveque and R. P. O'Connor, Nanosecond pulsed electric fields depolarize transmembrane potential via voltage-gated K(+), Ca(2 +) and TRPM8 channels in U87 glioblastoma cells, *Biochim. Biophys. Acta, Biomembr.*, 2017, **1859**(10), 2040–2050.

182 N. Todorova, C. Chiappini, M. Mager, B. Simona, II Patel, M. M. Stevens and I. Yarovsky, Surface presentation of functional peptides in solution determines cell internalization efficiency of TAT conjugated nanoparticles, *Nano Lett.*, 2014, **14**(9), 5229–5237.

183 E. Koren and V. P. Torchilin, Cell-penetrating peptides: breaking through to the other side, *Trends Mol. Med.*, 2012, **18**(7), 385–393.

184 K. Kim and W. G. Lee, Electroporation for nanomedicine: A review, *J. Mater. Chem. B*, 2017, **5**(15), 2726–2738.

185 B. Wang, J. Zhang, Y. Zhang, Z. Mao, N. Lu and Q. H. Liu, The penetration of a charged peptide across a membrane under an external electric field: A coarse-grained molecular dynamics simulation, *RSC Adv.*, 2018, **8**(72), 41517–41525.

186 S. Krause and B. L. Feringa, Towards artificial molecular factories from framework-embedded molecular machines, *Nat. Rev. Chem.*, 2020, **4**(10), 550–562.

187 E. Kopperger, J. List, S. Madhira, F. Rothfischer, D. C. Lamb and F. C. Simmel, A self-assembled nanoscale robotic arm controlled by electric fields, *Science*, 2018, **359**(6373), 296–301.

This journal is © the Owner Societies 2022

Phys. Chem. Chem. Phys., 2022, **24**, 6327–6348 | 6347

188 B. Tam and O. Yazaydin, Design of electric field controlled molecular gates mounted on metal–organic frameworks, *J. Mater. Chem. A*, 2017, **5**(18), 8690–8696.

189 J. P. Durholt, B. F. Jahromi and R. Schmid, Tuning the electric field response of MOFs by rotatable dipolar linkers, *ACS Cent. Sci.*, 2019, **5**(8), 1440–1448.

190 A. Knebel, B. Geppert, K. Volgmann, D. I. Kolokolov, A. G. Stepanov, J. Twiefel, P. Heitjans, D. Volkmer and J. Caro, Defibrillation of soft porous metal–organic frameworks with electric fields, *Science*, 2017, **358**(6361), 347–351.

191 J. Prusa and M. Cifra, Molecular dynamics simulation of the nanosecond pulsed electric field effect on kinesin nanomotor, *Sci. Rep.*, 2019, **9**(1), 19721.

192 D. Biriukov and Z. Futera, Adsorption of amino acids at the gold/aqueous interface: Effect of an external electric field, *J. Phys. Chem. C*, 2021, **125**(14), 7856–7867.

193 P. D. Raiter, Y. Vidavsky and M. N. Silberstein, Can polyelectrolyte mechanical properties be directly modulated by an electric field? A molecular dynamics study, *Adv. Funct. Mater.*, 2020, **31**(4), 2006969.

194 J. W. Ponder, C. Wu, P. Ren, V. S. Pande, J. D. Chodera, M. J. Schnieders, I. Haque, D. L. Mobley, D. S. Lambrecht, R. A. DiStasio, Jr., M. Head-Gordon, G. N. Clark, M. E. Johnson and T. Head-Gordon, Current status of the AMOEBA polarizable force field, *J. Phys. Chem. B*, 2010, **114**(8), 2549–2564.

195 H. Li, J. Chowdhary, L. Huang, X. He, A. D. MacKerell, Jr. and B. Roux, Drude polarizable force field for molecular dynamics simulations of saturated and unsaturated zwitterionic lipids, *J. Chem. Theory Comput.*, 2017, **13**(9), 4535–4552.

196 F. Y. Lin, J. Huang, P. Pandey, C. Rupakheti, J. Li, B. T. Roux and A. D. MacKerell, Jr., Further optimization and validation of the classical drude polarizable protein force field, *J. Chem. Theory Comput.*, 2020, **16**(5), 3221–3239.

197 J. A. Lemkul, J. Huang, B. Roux and A. D. MacKerell, Jr., An empirical polarizable force field based on the classical drude oscillator model: Development history and recent applications, *Chem. Rev.*, 2016, **116**(9), 4983–5013.

198 Z. Jing, C. Liu, S. Y. Cheng, R. Qi, B. D. Walker, J. P. Piquemal and P. Ren, Polarizable force fields for biomolecular simulations: recent advances and applications, *Annu. Rev. Biophys.*, 2019, **48**, 371–394.

6348 | *Phys. Chem. Chem. Phys.*, 2022, **24**, 6327–6348

This journal is © the Owner Societies 2022